

# 105, Rev. B

## Atmospheric and Environmental Effects

Released May 26, 2006

---

Document Owner:

Stephen Slobin

Stephen Slobin  
Antenna System Engineer

5-26-06

Date

Approved by:

Timothy T. Pham

DSN Chief System Engineer

5/8/06

Date

Released by:

[Signature on file]

5/26/2006

DSMS Document Release

Date

## *Change Log*

<b>Rev</b>	<b>Issue Date</b>	<b>Affected Paragraphs</b>	<b>Change Summary</b>
Initial	11/30/2000	All	All
A	12/15/2002	All	Provides monthly weather statistics for all stations and frequency bands
B	5/26/2006	2.1, 2.4	Revised weather models, provides new methods for calculating system operating noise temperature and planetary noise effects

## *Note to Readers*

There are two sets of document histories in the 810-005 document that are reflected in the header at the top of the page. First, the overall document is periodically released as a revision when major changes affect a majority of the modules. For example, this document is part of Revision E. Second, the individual modules also change, starting as the initial issue that has no revision letter. When a module is changed, a change letter is appended to the module number on the second line of the header and a summary of the changes is entered in the module's change log.

## ***Contents***

<b><u>Paragraph</u></b>	<b><u>Page</u></b>
1 Introduction.....	6
1.1 Purpose.....	6
1.2 Scope.....	6
2 General Information .....	7
2.1 Atmospheric Attenuation and Noise Temperature .....	7
2.1.1 Calculation of Mean Atmospheric Physical Temperature .....	9
2.1.2 Elevation Angle Modeling .....	10
2.1.3 Calculation of Noise Temperature From Attenuation.....	10
2.1.4 Cosmic Background Adjustment .....	11
2.1.5 Example of Use of Attenuation Statistics to Calculate Atmospheric Noise Temperature, $T_{\text{atm}}(\text{CD}, \theta)$ , and $T_{\text{op}}(\text{CD}, \theta)$ .....	12
2.1.6 Best/Worst Month Ranges of Atmospheric Noise Temperature and Attenuation .....	13
2.2 Rainfall Statistics.....	14
2.3 Wind Loading.....	14
2.4 Hot Body Noise .....	15
2.4.1 Solar Noise .....	15
2.4.2 Lunar Noise .....	18
2.4.3 Planetary Noise .....	19
2.4.4 Galactic Noise.....	21

## ***Illustrations***

<b><u>Figure</u></b>	<b><u>Page</u></b>
1. Cumulative Distributions of Zenith Atmospheric Noise Temperature at L-Band and S-Band, Goldstone DSCC .....	22
2. Cumulative Distributions of Zenith Atmospheric Noise Temperature at L-Band and S-Band, Canberra DSCC.....	23
3. Cumulative Distributions of Zenith Atmospheric Noise Temperature at L-Band and S-Band, Madrid DSCC.....	24
4. Cumulative Distributions of Zenith Atmospheric Noise Temperature at X-Band, Goldstone DSCC .....	25

5.	Cumulative Distributions of Zenith Atmospheric Noise Temperature at X-Band, Canberra DSCC.....	26
6.	Cumulative Distributions of Zenith Atmospheric Noise Temperature at X-Band, Madrid DSCC.....	27
7.	Cumulative Distributions of Zenith Atmospheric Noise Temperature at Ka-Band, Goldstone DSCC .....	28
8.	Cumulative Distributions of Zenith Atmospheric Noise Temperature at Ka-Band, Canberra DSCC.....	29
9.	Cumulative Distributions of Zenith Atmospheric Noise Temperature at Ka-Band, Madrid DSCC.....	30
10.	Probability Distribution of Wind Conditions at Goldstone .....	31
11.	Solar Radio Flux at 2800 MHz (10.7 cm wavelength) During Solar Cycle 23 (1996–2007) .....	32
12.	DSS-15 HEF Antenna X-Band System Noise Temperature Increases Due to the Sun at Various Offset Angles, Showing Larger Increases Perpendicular to Quadripod Directions .....	33
13.	DSS-16 S-Band Total System Noise Temperature at Various Offset Angles from the Sun.....	34
14.	DSS-12 S-Band Total System Noise Temperature at Various Declination and Cross-Declination Offsets from the Sun.....	35
15.	DSS-12 X-Band Total System Noise Temperature at Various Declination and Cross-Declination Offsets from the Sun.....	36
16.	DSS-13 Beam-Waveguide Antenna X-Band Noise Temperature Increase Versus Offset Angle, March 1996.....	37
17.	DSS-13 Beam-Waveguide Antenna Ka-Band Noise Temperature Increase Versus Offset Angle, March 1996.....	37
18.	Total S-Band System Noise Temperature for 70-m Antennas Tracking Spacecraft Near the Sun (Derived from 64-m Measurements).....	38
19.	X-Band Noise Temperature Increase for 70-m Antennas as a Function of Sun-Earth-Probe Angle, Nominal Sun, 23,000 K Disk Temperature .....	39
20.	Normalized Temperature Increase for Half-power Beamwidth Diameter to Planetary Disk Diameter Ratios from 2.0 to 5.0.....	40

## ***Tables***

<b><u>Table</u></b>	<b><u>Page</u></b>
1. Cumulative Distributions of Zenith Atmospheric Noise Temperature at L- and S-Bands for Goldstone DS <sup>C</sup> C.....	41
2. Cumulative Distributions of Zenith Atmospheric Noise Temperature at L- and S-Bands for Canberra DS <sup>C</sup> C .....	42
3. Cumulative Distributions of Zenith Atmospheric Noise Temperature at L- and S-Bands for Madrid DS <sup>C</sup> C .....	43
4. Cumulative Distributions of Zenith Atmospheric Noise Temperature at X-Band for Goldstone DS <sup>C</sup> C.....	44
5. Cumulative Distributions of Zenith Atmospheric Noise Temperature at X-Band for Canberra DS <sup>C</sup> C .....	45
6. Cumulative Distributions of Zenith Atmospheric Noise Temperature at X-Band for Madrid DS <sup>C</sup> C .....	46
7. Cumulative Distributions of Zenith Atmospheric Noise Temperature at Ka-Band for Goldstone DS <sup>C</sup> C.....	47
8. Cumulative Distributions of Zenith Atmospheric Noise Temperature at Ka-Band for Canberra DS <sup>C</sup> C .....	48
9. Cumulative Distributions of Zenith Atmospheric Noise Temperature at Ka-Band for Madrid DS <sup>C</sup> C .....	49
10. Cumulative Distributions of Zenith Atmospheric Attenuation at L- and S-Bands for Goldstone DS <sup>C</sup> C.....	50
11. Cumulative Distributions of Zenith Atmospheric Attenuation at L- and S-Bands for Canberra DS <sup>C</sup> C .....	51
12. Cumulative Distributions of Zenith Atmospheric Attenuation at L- and S-Bands for Madrid DS <sup>C</sup> C .....	52
13. Cumulative Distributions of Zenith Atmospheric Attenuation at X-Band for Goldstone DS <sup>C</sup> C .....	53
14. Cumulative Distributions of Zenith Atmospheric Attenuation at X-Band for Canberra DS <sup>C</sup> C .....	54
15. Cumulative Distributions of Zenith Atmospheric Attenuation at X-Band for Madrid DS <sup>C</sup> C.....	55
16. Cumulative Distributions of Zenith Atmospheric Attenuation at Ka-Band for Goldstone DS <sup>C</sup> C .....	56

17. Cumulative Distributions of Zenith Atmospheric Attenuation at Ka-Band for Canberra DSCL.....	57
18. Cumulative Distributions of Zenith Atmospheric Attenuation at Ka-Band for Madrid DSCL.....	58
19. Monthly and Year-Average Rainfall Amounts at the DSN Antenna Locations .....	59
20. Parameters for X-Band Planetary Noise Calculation, plus X-Band and Ka-Band Noise Temperatures at Mean Minimum Distance from Earth.....	60

# **1      *Introduction***

## **1.1      *Purpose***

This module provides sufficient information concerning atmospheric, environmental, and extraterrestrial effects to enable a flight project to design a telecommunications link at the L-, S-, X-, and Ka-band frequencies used by the DSN.

## **1.2      *Scope***

Statistics of atmospheric attenuation and noise temperature at each tracking antenna site are presented for those microwave frequencies used by the DSN. In this module, the values of attenuation and noise temperature increase are given relative to a no-atmosphere (vacuum) condition, thus this presentation is compatible for use with the vacuum gain and noise temperature presentations of antenna performance given in modules 101 for 70-m antennas, 102 for 26-m antennas, 103 for 34-m high-efficiency (HEF) antennas, and 104 for 34-m beam-waveguide (BWG) antennas.

Statistics of wind speed at Goldstone are given. These are used both to determine the statistics of antenna gain reduction due to wind loading and also to ascertain the percentage of time an antenna will be unusable due to excessive wind speed.

Extraterrestrial effects are primarily the increased system noise temperature due to hot body noise from the Sun, Moon, planets, and galactic radio sources. These effects are significant only when the antenna beam is in the vicinity of these noise sources during tracking of spacecraft.

Charged-particle effects are given in module 106, Solar Corona and Solar Wind Effects.

## 2      *General Information*

### 2.1      *Atmospheric Attenuation and Noise Temperature*

The principal weather-related effects on telecommunications link performance are the atmospheric attenuation and noise temperature resulting from oxygen, water vapor, clouds, and rain. The two effects are related and higher atmospheric attenuation produces a higher noise contribution. Also, atmospheric effects generally increase with increasing frequency, except in the vicinity of the water vapor line at 22.235 GHz (20-25 GHz), and the oxygen band from about 55-65 GHz. Ka-band effects are larger than X-band effects, which in turn are larger than S-band and L-band effects.

In the 810-005 antenna performance modules (modules 101, 102, 103, and 104), *effective antenna gain* (vacuum gain minus atmospheric attenuation) is presented in the figures for various atmospheric attenuation values. Strictly speaking, the gain of an antenna is not a function of atmospheric attenuation; however for stand-alone use, the effective gain, including atmospheric loss, is a useful concept, and the expressions for gain in the appendices of those modules include a term for atmospheric attenuation. Similarly, the *antenna temperature* (due to spillover, LNA contribution, waveguide loss, etc.) is also not a function of atmosphere. However, the operating noise temperature as presented in the appendices of the antenna performance modules includes a term for atmospheric noise contribution. The vacuum system noise temperature as given in those modules also includes the constant 2.725 K contribution from the cosmic background, which adds to the basic antenna temperature value. An alternate formulation of antenna noise characterization,  $T_{AMW}$  (due to antenna and microwave contributions only), is being phased into the antenna modules, and a description of that term and its use is given in this module.

Design control tables (DCTs) used for telecommunications link design typically carry separate entries for atmospheric attenuation of the received or transmitted signal and atmospheric noise contribution as a function of elevation angle and weather condition. It is important in those DCTs that the antenna gain and system operating noise temperature values reflect the vacuum performance of the antenna by itself, so as to prevent double-bookkeeping of the atmospheric attenuation and noise temperature contributions.

Three atmospheric models are presented here. The first covers L-band (1.7 GHz) and S-band (2.3 GHz). The other two cover X-band (8.4 GHz), and Ka-band (32.0 GHz). Atmospheric noise temperature and attenuation statistics are provided in the form of cumulative distributions (CDs) for each effect. For example, a cumulative distribution of 0.90 ("90% weather") means that 90% of the time a particular weather effect (noise temperature or attenuation) is less than or equal to a given value. Conversely, that particular effect is exceeded 10% of the time. Qualitatively, the weather conditions associated with selected cumulative distributions are described as follows:

CD = 0.00	clear dry, lowest weather effect
CD = 0.25	average clear weather

CD = 0.50	clear humid, or very light clouds
CD = 0.90	very cloudy, no rain
CD > 0.95	very cloudy, rain

By their very natures, clouds and rain are poorly modeled, and the water vapor radiometer data used here are sparse for the larger rain-related weather effects, which are exceeded only 5% of the time.

The Ka-band model presented here is based on actual water vapor radiometer zenith noise temperature measurements made at 31.4 GHz at all three DSN sites (Goldstone, Canberra, and Madrid). Used in the modeling were 101 months of Goldstone data covering the period October 1993 through July 2005, 70 months of Canberra data covering the period June 1999 through July 2005, and 147 months of Madrid data covering the period September 1990 through July 2005. There were missing months of data from each station. Note also that different numbers of months of data went into the model for each of the separate months (for example, there may have been 12 Februaries, but only 10 Marches). It is felt that because of the large amount of Madrid data (more than 12 years), the results will fairly accurately represent true long-term statistics. The 8-1/2 years of Goldstone data will give a moderately accurate long-term model. The nearly 6 years of Canberra data will probably not give a very accurate long-term model, and future updates of the Canberra model may show relatively large changes in the distributions. Cumulative distributions at 31.4 GHz for each of the 12 months were calculated, then increased by a small amount (0.3 – 3 K, a function of frequency and noise temperature) to create a model for 32 GHz. A year-average model was developed by calculating the weighted-average noise temperature of all the 12 months, at each CD level.

L/S-band and X-band attenuation statistics were created from the Ka-band (32 GHz) statistics by subtracting out the 0% CD baseline (calculated for nominal temperatures and pressures, with 0% relative humidity), frequency-squaring to the appropriate frequency (for example,  $[8.42/32]^2$ ) and then adding in the 0% CD baseline at the new frequency. Note that the 0% CD baselines for the DSN sites differ because of different heights above sea level. Noise temperature statistics were then derived from the frequency-modeled attenuation statistics.

Noise temperature statistics for zenith were created from the atmospheric attenuation statistics by methods given in Sections 2.1.1 and 2.1.3 below. The year-average noise temperature statistics were calculated from the year-average attenuation values rather than by calculating the average of all the monthly noise temperatures. These two methods give very slightly different results.

It should be noted that although the noise temperature statistics are the best qualitative measures for comparison of different locations and different frequencies, especially when dealing with low-noise systems (where the atmospheric noise is a large part of the total system noise temperature), the basic data base for the calculation of atmospheric effects is actually the attenuation statistics. Given a station location, frequency, and CD of interest, the attenuation data base value is extracted, modeled to the elevation angle of interest (Section 2.1.2), and then the appropriate atmospheric noise temperature is calculated (Section 2.1.3). Monthly, year-average, and maximum and minimum monthly zenith noise temperature statistics

are given in Tables 1 through 9. Similarly, the attenuation statistics are given in Tables 10 through 18.

The atmospheric models thus generated for a particular complex (for example, Goldstone) should be used for all antennas at that complex (for example, DSS-14, DSS-15, DSS-24, etc.), regardless of the small altitude differences among the antennas.

Zenith atmospheric noise temperature statistics for the three DSN sites at L- and S-band are provided in Tables 1 through 3. Tables 4 through 6 provide similar statistics for X-band, and Tables 7 through 9 cover Ka-band. The tables include the maximum and minimum monthly value for each CD level, the year average for that CD level and the average value for each month. These noise temperature statistics should be used only in a qualitative sense to describe the relative levels of atmospheric noise contributions at different locations and cumulative distributions. They should not be used for elevation modeling as this is properly performed using the calculated attenuation at a given elevation angle as a starting point and following the process that is described below.

The use of these statistics depends on the context in which the antenna temperature is stated. When a nominal antenna zenith  $T_{op}$  (operating system noise temperature) is stated, it is considered to include the CD = 25% (average clear sky) value for the appropriate frequency and location. However, “vacuum” antenna temperatures, which include cosmic noise contribution, are sometimes used to describe the performance of an antenna independent of location. In this case the operating system noise temperature should be referred to as  $T_{op, vac}$ .

Tables 10 through 18 provide similar presentations for zenith atmospheric attenuation. The tolerances of atmospheric noise temperature and attenuation, as given in Tables 1 through 18, should be considered to be 5% of the stated values at zenith, or 5% of the values calculated for elevation angles other than zenith. (see Section 2.1.5, below).

Figures 1, 2, and 3 show the L/S-band noise temperature statistics for Goldstone, Canberra, and Madrid respectively. Figures 4, 5, and 6 show X-band statistics for the three complexes. Figures 7, 8, and 9 provide the Ka-band statistics. On each figure, the year-average cumulative distribution, the minimum envelope value, and the maximum envelope values are given for all the individual months at each CD value stated in Tables 1 through 9. Curves of zenith attenuation are not given, although using a rule-of-thumb that a medium with 1 dB attenuation at a physical temperature of about 20 C radiates a noise temperature of approximately 60 K, the Ka-band curves can be used to make rough estimates of the zenith attenuation at the various frequencies. This relationship is nearly linear over the range from 0 to 1 dB.

For other nearby frequencies to the L-, S-, X-, and Ka-bands, the weather-effects models presented here should be used without modification. These models should definitely not be used to infer statistics in the vicinity of the 22.235 GHz water vapor line (20-25 GHz) or the 60 GHz oxygen band, 55-65 GHz.

### 2.1.1 *Calculation of Mean Atmospheric Physical Temperature*

The mean physical temperature of the atmosphere is modeled to be a function of the cumulative distribution of weather effects. This reflects the assumption that those effects that

are of larger value (for example, high noise temperature) occur closer to the surface (for example, rain, low moist clouds) and hence are at a higher average physical temperature than those that have a lesser effect (a clear sky with low humidity). The mean atmospheric physical temperature is modeled as

$$T_p = 255 + 25 \times CD, \text{ K} \quad (1)$$

where

$CD$  = cumulative distribution of weather effect ( $0.0 \leq CD \leq 0.99$ ).

Note that the maximum value of  $T_p$  thus becomes nearly 280 K, or about 7 C.

### 2.1.2 *Elevation Angle Modeling*

Only the attenuation should be modeled as a function of elevation angle. The atmospheric noise temperature contribution at any elevation angle can be calculated from the modeled attenuation at that elevation angle. Elevation angle modeling can be performed using either a flat-Earth or a round-Earth model. A flat-Earth model is used here, wherein the attenuation increases with decreasing elevation angle:

$$A(\theta) = A_{zen} \times AM = \frac{A_{zen}}{\sin(\theta)}, \text{ dB} \quad (2)$$

where

$\theta$  = elevation angle of antenna beam

$A_{zen}$  = zenith atmospheric attenuation (dB), as given Tables 10 through 18 of this module

$AM$  = number of air masses  $\left( \frac{1}{\sin(\theta)} = 1.0 \text{ at zenith} \right)$

The flat-Earth approximation produces a slightly higher attenuation than would be obtained with a round-Earth model for low elevation angles but is valid to within 1% to 3% at a 6-deg elevation angle, depending on the frequency and the amount of water vapor in the atmosphere. Note that in a telecom link design tool, if the atmosphere attenuation is carried as a separate line item, it should NOT also be included in the "effective" antenna gain (antenna gain minus atmosphere attenuation).

### 2.1.3 *Calculation of Noise Temperature From Attenuation*

An attenuating atmosphere creates a noise temperature contribution to ground antenna system temperature. The atmospheric noise temperature at any elevation angle ( $\theta$ ) is calculated from the attenuation by

$$T_{atm}(\theta) = T_p \left[ 1 - \frac{1}{L(\theta)} \right], \text{ K} \quad (3)$$

where

$T_p$  = mean physical temperature of atmosphere (K), calculated above

$L(\theta)$  = loss factor of atmosphere =  $10^{\left[ \frac{A(\theta)}{10} \right]}$

$A(\theta)$  = atmospheric attenuation at any elevation angle (dB), calculated above

Note that typical values of  $L$  range from about 1.01 to 2.0 ( $A=0.04$  dB to 3 dB)

#### 2.1.4 Cosmic Background Adjustment

The noise temperature contribution of the cosmic microwave background is reduced by atmospheric attenuation. For all DSN frequencies the cosmic background noise temperature before atmospheric attenuation is

$$T_{CMB} = 2.725 \text{ K} \quad (4)$$

With atmosphere attenuation, the effective cosmic background becomes

$$T'_{CMB}(\theta) = \frac{T_{CMB}}{L(\theta)}, \text{ K} \quad (5)$$

where

$T_{CMB}$  = cosmic microwave background noise (K) without atmosphere

$L(\theta)$  = loss factor of atmosphere at the elevation angle of interest, as calculated from Section 2.1.3.

The expressions for  $T_{op}$  in the telecommunications interface modules (for example, module 104 Rev. B, Appendix A) include an attenuated cosmic contribution (effective cosmic background above) associated with the coefficients  $T_1$  and  $T_2$ . These terms define what is commonly referred to as the *vacuum noise temperature* of the antenna, without atmosphere contribution, but including a cosmic contribution. This effective background noise is typically within a few tenths of a kelvin of the  $T_{CMB}$  value given above, and variations in the  $T'_{CMB}$  value as a function of weather condition and elevation angle are neglected, as being at the sub-1K level. As such, the equations for  $T_{op}$  in modules 101 Rev. A, 102, 103, and 104 Rev. B should be used with the  $T_1$  and  $T_2$  values as given in their respective Appendices.

Future revisions of these telecommunications interface modules will present a different formulation for system operating noise temperature. The system operating noise

temperature,  $T_{op}$ , will consist of two parts – an *antenna-microwave* component,  $T_{AMW}$ , for the contribution of the antenna and microwave hardware, and a *sky* component,  $T_{sky}$ , that will consist of the atmosphere noise plus the cosmic microwave background noise, attenuated by the atmosphere loss. New  $T_1$  and  $T_2$  coefficients will be given in the Appendices of the antenna modules, and the appropriate equation to use will also be stated. Thus, for the revisions, the system operating noise temperature with atmosphere and with attenuated cosmic contribution becomes

$$T_{op}(\theta) = T_{AMW} + T_{sky} = [T_1 + T_2 e^{-a\theta}] + [T_{atm}(\theta) + T'_{CMB}(\theta)] \quad (6)$$

where

$T_1$ ,  $T_2$  and  $a$  are coefficients from the telecommunications interface modules

$T_{atm}$  is the atmosphere contribution term,

$T'_{CMB}$  is given above

### 2.1.5 Example of Use of Attenuation Statistics to Calculate Atmospheric Noise Temperature, $T_{atm}(CD, \theta)$ , and $T_{op}(CD, \theta)$

The following example will show a typical calculation of atmospheric attenuation and noise temperature for a particular situation. The parameters for the example are

DSS-43, Canberra

Ka-band (32 GHz)

90% year-average weather (CD = 0.90)

20-deg elevation angle (2.924 air masses)

From Table 17, the year-average zenith attenuation for CD = 0.90 is given as

$$A_{zen} = 0.396 \text{ dB.}$$

The attenuation at 20-deg elevation is

$$A(90\%, 20^\circ) = \frac{0.396}{\sin(20)} = 1.158 \text{ dB}$$

Note that in a telecom link design tool, if the atmosphere attenuation is carried as a separate line item, it should NOT also be included in the *effective antenna gain* (antenna gain minus atmosphere attenuation).

The loss factor  $L$  at 20-deg elevation is

$$L(90\%, 20^\circ) = 10^{1.158/10} = 1.306$$

The atmospheric mean physical temperature is

$$T_p = 255 + 25 \times 0.90 = 277.5 \text{ K}$$

The atmospheric noise temperature at 20-deg elevation is

$$T_{atm}(90\%, 20^\circ) = 277.5 \left[ 1 - \frac{1}{1.306} \right] = 65.019 \text{ K}$$

The effective cosmic background temperature at 20-deg elevation is

$$T'_{CMB} = \frac{2.725}{1.306} = 2.087 \text{ K}$$

The operating system noise temperature at 20-deg elevation is

$$T_{op}(90\%, 20^\circ) = T_{AMW}(20^\circ) + 65.019 + 2.087 = T_{AMW}(20^\circ) + 67.106 \text{ K}$$

where

$T_{AMW}(\theta)$  is obtained from revisions of the telecommunications interface modules published after May, 2006.

The “old” (before May, 2006) formulation in the telecommunications interface modules includes the cosmic microwave background in  $T_{op,vac}(\theta)$ , and the operating system noise temperature at any elevation angle for any weather condition is given by

$$T_{op}(CD, \theta) = T_{op,vac}(\theta) + T_{atm}(CD, \theta), \text{ K} \quad (7)$$

where

$T_{op,vac}(\theta)$  is obtained from revisions of the telecommunications interface modules published before May, 2006.

For this example using the old formulation, the operating system noise temperature at 20-deg elevation is

$$T_{op}(90\%, 20^\circ) = T_{op,vac}(20^\circ) + T_{atm}(90\%, 20^\circ) = T_{op,vac}(20^\circ) + 65.019 \text{ K}$$

## 2.1.6 Best/Worst Month Ranges of Atmospheric Noise Temperature and Attenuation

Although the absolute accuracy of the 31.4-GHz water vapor radiometer measurements used to create the noise temperature statistics is thought to be on the order of the values stated in paragraph 2.1 (a few tenths K to 2 K at zenith, depending on CD), the month-to-month variation of average noise temperature at any CD varies much more than this at all values of cumulative distribution greater than about 10%. A particular month might be the “worst” at the 90% CD level, but merely “moderate” at lower CD levels. An example is a winter month that has a large amount of rain but when not raining has low humidity and low noise temperature

contribution. At this time, there are insufficient data to characterize "best" and "worst" months individually; however, tolerances on the mean statistics as given in Tables 1 through 18 can give the user a feeling of what yearly variations in atmospheric effects may be expected.

Inspection of Tables 1 through 18 and Figures 1 through 9 will show that fictitious "best month" and "worst month" statistics can be generated from the values giving the minimum and maximum envelope values of noise temperature and attenuation, without regard to the variability among the months as a function of CD. At high values of CD, the adverse (maximum envelope) yearly tolerances can be as high as 40% of the year-average value of an effect. It should be noted that adverse tolerances for both noise temperature and attenuation give INCREASES from the values in Tables 1 through 18. An adverse VALUE is a mean PLUS the adverse tolerance. For mission planning purposes, with no need to create a model for a specific month, it may be sufficient to use the year-average value at a particular CD, and use the maximum/minimum envelope values to define very conservative (large) adverse/favorable tolerances, with triangular distribution. For specific-month planning purposes, it may be sufficient to use the values given in Tables 1 through 18, with  $\pm 5\%$  tolerances (triangular distribution) as stated above. A very conservative approach (acknowledging that any individual month in the future can be well outside the historical range of available data) would be to use the "maximum" envelope as the model for a possible "bad" month. Note also that for particular months characterized by "bad weather", year-to-year variation of noise temperature and attenuation statistics can be quite large.

## 2.2 *Rainfall Statistics*

To assist the user in determining which months may have large rainfall-related atmospheric noise temperature and attenuation increases, rainfall data are presented for the three DSN antenna locations. Months with large average rainfall amounts may not necessarily correspond to months with large noise temperature and attenuation values. Comparison with Tables 1 through 18 should be made.

Table 19 presents the monthly and year-average rainfall amounts for the three DSN antenna locations. The Goldstone data (1973–2000) were taken at the administration center, located near the middle of the Goldstone antenna complex. Some antennas may be located as much as 10 miles from this location. The Canberra data (1966–2002) were taken at the Tidbinbilla Nature Reserve, located about 3 miles southwest of the antenna site. The Madrid data (1961–1990) are the averages of the rainfall at two locations: Avila, about 20 miles northwest of the antenna site, and Madrid (Quatro Vientos) about 20 miles east of the antenna site. Although these averages may not exactly reflect the rainfall at the antenna site, the relative monthly amounts are undoubtedly correct.

## 2.3 *Wind Loading*

The effect of wind loading must be modeled probabilistically, since wind velocity varies randomly over time and space. Figure 10 shows the probability distribution of wind speed for Goldstone. Similar data for the Madrid and Canberra complexes will be supplied when available. The wind load on a particular antenna is dependent on the design of that antenna.

Consequently, information about wind-load effect on antenna gain is listed in the appropriate antenna module.

Statistics show that Goldstone is the windiest of the three Deep Space Network antenna complexes. The DSS-14 70-m antenna is *stowed* (pointed vertically) when wind gusts exceed 55 mph (88 km/hr). The frequency of occurrence of this event can be deduced from a relationship between wind gusts and average wind speed. This relationship is found to be: maximum hourly wind speed =  $0.62 \times$  strongest gust. Thus, for 55-mph (88 km/hr) gusts, the maximum hourly wind speed is found to be 34 mph (55 km/hr). From Figure 10, it is seen that this speed is exceeded approximately 2 % (175 hours) of the year and 4 % (29 hours) of the worst month. Actual practice has shown that no antenna has been stowed more than about 10 hours per year due to excessive wind-gust occurrences.

## 2.4        ***Hot Body Noise***

### 2.4.1      ***Solar Noise***

The increase in system noise when tracking near the Sun depends on the intensity of solar radiation at the received frequency and on the position of the Sun relative to the antenna gain pattern. The subreflector support structure (typically a quadripod, but a tripod at the DSS-13 BWG antenna) introduces non--uniformities in the sidelobe structure. Increases in noise temperature are typically greater in directions at right angles to the planes established by the subreflector support legs and the center of the reflector surface. Thus, a quadripod-type antenna will have four enhanced regions of noise temperature, and a tripod-type antenna will have six. With an azimuth-elevation (AZ-EL) or X-Y mounted antenna, the plane containing the Sun-Earth-Probe (SEP) angle will rotate through the sidelobes during a tracking pass. This causes the solar noise to fluctuate during a track even if the SEP angle is constant.

A large number of measurements were made at Goldstone from 1987 to 1996 to determine the system noise temperature effects of tracking near the Sun (within about five deg from the center of the solar disk). These measurements were made at S-band on the 26-m antennas and at S-, X-, and Ka-bands on the 34-meter antennas.

Figure 11 shows the 10.7-cm (2800-MHz) solar radio flux during solar cycle 23 (1996-2007, with the maximum occurring in late 2001). The flux is measured in solar flux units (SFU) where one SFU =  $1 \times 10^{-22} \text{ W/m}^2/\text{Hz}$ . Updated solar flux predictions can be found at the National Oceanic and Atmospheric Administration (NOAA) Space Environment Center web site <<http://www.sec.noaa.gov/weekly.html>> (Solar Cycle Progression and Prediction Plots). Solar flux predictions can be used to model S- and X-band solar noise temperature contributions using the ratio of predicted solar flux to the solar flux that existed at the time the antenna noise temperatures were measured.

The general characteristic of the 11-year cycle of 2800-MHz solar flux is a rapid rise to a peak approximately 4–5 years after the minimum, followed by a 7–6 year gradual decrease. From cycle to cycle, the peak flux can vary by as much as a factor of two. The 10.7-cm flux varied during solar cycle 23 from a minimum of about 70 SFU during 1996 to a maximum

of about  $225 \pm 15$  SFU in late 2001 and will return to an expected minimum of about 70 SFU during early 2007.

Figure 12 shows X-band system noise temperature increases as measured at the Goldstone DSS-15 HEF antenna. These measurements show the increased effect for the Sun located (offset) at right angles to the quadripod legs. The quadripod legs are arranged in an “X” configuration, with 90-deg spacing. The measurements were made in November 1987 (near the beginning of the solar cycle) with a measured 2800-MHz flux value of 101 SFU and an 8800-MHz flux value of 259 SFU. The following expression may be used as an upper limit of X-band solar noise contribution at DSS-15 as shown in Figure 12.

$$T_{\text{sun}} = 800e^{-2.0\theta}, \text{ K} \quad (8)$$

where

$$\theta = \text{offset angle between center of beam and center of solar disk, deg}$$

Figure 13 shows S-band (2295 MHz) total system noise temperature measurements made on the Goldstone DSS-16, 26-m antenna on December 20, 1989. This antenna has no quadripod, and it can be assumed that the noise temperature values shown are independent of solar “clock angle” around the center of the antenna beam. The reported 2800-MHz solar flux at the time of the experiment was 194 SFU; at 8800 MHz it was 290 SFU. Note that compared to the November 1987 flux (Figure 12), the 2800-MHz flux has nearly doubled, but the 8800-MHz flux has only increased about 12 percent. The S-band solar contribution shown in Figure 13 can be modeled as

$$T_{\text{sun}} = 1400e^{-1.4\theta}, \text{ K} \quad (9)$$

where

$$\theta = \text{offset angle between center of beam and center of solar disk, deg}$$

Figures 14 and 15 are contour plots of the DSS-12, 34-m HA-DEC total system noise temperature versus declination and cross-declination antenna pointing offsets. DSS-12 has been decommissioned since the measurements were made, but the figures are included because they are representative of the effects of the quadripod on solar noise at other antennas. The quadripod legs are arranged in a “+” configuration with 90-deg spacing, hence the peaks at right angles to the legs.

Figure 14 is a contour plot of total S-band system noise temperature versus declination and cross-declination antenna pointing offsets at DSS-12. The contour interval is 50 K. These measurements were made on January 12, 1990. On this day the reported 2800-MHz solar flux was 173 SFU.

Figure 15 is a contour plot of total X-band system noise temperature versus declination and cross-declination antenna pointing offsets at DSS-12. The contour interval,

measurement date, and flux values are identical with those in Figure 14. The reported 8800-MHz solar flux was 272 SFU.

Figures 16 and 17 show the X-band (8.4-GHz) and Ka-band (32-GHz) solar noise contributions at the DSS-13, 34-m research and development beam waveguide antenna as a function of offset angle from the center of the sun. These data were taken during mid-March, 1996, when the 10.7-cm solar flux was about 70 SFU (the minimum at the end of solar cycle 22 and at the beginning of solar cycle 23) and should be considered as representative of what is expected at the operational DSN beam waveguide antennas.

The following expressions give an approximate upper envelope for the noise contributions shown in Figures 16 and 17 as a function of offset angle

$$T_{\text{sun}} = \begin{cases} 1400e^{-5.1\theta}, & 0.35 < \theta \leq 0.75 \text{deg} \\ 86e^{-1.4\theta}, & \theta > 0.75 \text{deg} \end{cases}, \text{ at X-band} \quad (10)$$

$$T_{\text{sun}} = \begin{cases} 5000e^{-6.6\theta}, & 0.35 < \theta \leq 0.75 \text{deg} \\ 100e^{-1.4\theta}, & \theta > 0.75 \text{deg} \end{cases}, \text{ at Ka-band.} \quad (11)$$

At offset angles less than 0.35 deg (0.08 deg from the edge of the solar disk), solar noise contributions are likely to be in excess of 300 K at both frequencies. At offsets greater than 4.0 degrees, the solar contribution is negligible.

All noise contribution expressions given above should be compared with values shown in the corresponding figures to assess their validity. Note that these expressions should be considered valid only for the flux values given at the time of measurement. For predictive purposes, Figure 11 may be used to obtain future predicted 2800-MHz solar flux, and the noise contributions at S- and X-band can be modeled as described below.

During the 11-year solar cycle, the S-band flux varies by a factor of 3 (reference Figure 11) while the corresponding X-band flux varies by a factor of 2. For cycle 23, when the S-band range is expected to be from 70 SFU to as much as 210 SFU, the X-band range is predicted to be from about 200 SFU to about 400 SFU. The predicted X-band flux can be derived from the predicted S-band flux by the following expression.

$$\text{FLUX, X} = 200 + \frac{200(\text{FLUX, S} - 70)}{140} \quad (12)$$

For example, in January 2003 the mean S-band flux is predicted to be 125 SFU (from Figure 11). The mean predicted X-band flux would be 264 SFU.

The predicted solar noise contribution can be calculated based on measured noise contributions described above. For example, using the equation provided for Figure 12 (Equation 8) and the predicted X-band solar flux in January of 2002 (264 SFU), the predicted X-band solar noise contribution for a 2-degree offset angle using the 34-m HEF antenna would be

$$T_{\text{sun}} = \frac{264}{259} 800 e^{-2.0 \times 2.0} = 14.6 \text{ K} \quad (13)$$

At Ka-band, the solar flux varies little over the solar cycle and the relationship between noise temperature increase and offset angle depicted in Figure 17 can be used at all times.

Figure 18 shows examples of measured S-band system noise temperature made with a 64-m antenna tracking Pioneer 8 (November 1968, near the solar maximum) and Helios (April 1975, near the solar minimum). For all practical purposes, these curves may be used to predict S-band performance for the DSN 70-m antennas. The “maximum” and “minimum” curves for each month show the solar “clock angle” effect due to sidelobes at right angles to the quadripod legs.

Figure 19 shows a theoretical curve of X-band 70-m antenna noise temperature as a function of SEP angle. This curve is generated based on an assumed X-band blackbody disk temperature of 23,000 K, representing an “average” value during the solar cycle. An expression giving quiet Sun brightness temperature,  $T_b$  (K), as a function of wavelength (mm) has been found to be

$$T_b = 5672 \lambda^{0.24517}, \quad \text{K} \quad (14)$$

For S-band (2.3 GHz),  $T_b = 18700$  K. For X-band (8.5 GHz)  $T_b = 13600$  K. For Ka-band (32 GHz)  $T_b = 9750$  K. The active Sun may be expected to have an X-band brightness temperature of as much as two to four times as high as the 13600 K calculated above.

#### 2.4.2 *Lunar Noise*

For an antenna pointed near the Moon, a noise temperature determination similar to that made for the Sun should be carried out. The blackbody disk temperature of the Moon is about 240 K at X- and Ka-bands, somewhat lower at S-band (220 K), and its apparent diameter is almost exactly that of the Sun's (approximately 0.5 deg). Figures 12 through 19 may be used for lunar calculations, with the noise temperature values scaled by 240/23000. Figures 13, 14, 15, and 18 include clear-sky system noise temperatures, which must be subtracted out before scaling in order to determine the lunar noise temperature increase. Nevertheless, at offset angles greater than 2 deg, the lunar noise contribution is negligible. For rough calculations using antenna patterns with half-power beamwidths less than about 20% of the lunar diameter (all DSN antennas at X- and Ka-bands and the 70-m antennas at S-band), more than 90% of the antenna power is on the lunar disk when centered on the moon. In this case, the maximum noise temperature seen is roughly

$$T_{\text{moon}} = T_b \times 0.90 \times \eta_{\text{ant}}$$

where

$$T_b = 240 \text{ K}$$

$\eta_{ant}$  = antenna efficiency  $\approx 0.70$  for most large antennas

Thus, the peak noise contribution from the moon for any DSN antenna except the 34-m BWG antenna at S-band will be approximately 150 K. Measurements on the DSS-13 34-m beam waveguide antenna (S-band half-power beamwidth  $\approx 0.25$  deg) yield a noise temperature increase due to the moon of about 135 K.

#### 2.4.3 Planetary Noise

The increase in system noise temperature when tracking near a planet can be calculated by the formula

$$T_{pl} = \left( \frac{T_k G d^2}{16 R^2} \right) e^{-2.77 \left( \frac{\theta}{\theta_0} \right)^2}, \text{ K} \quad (15)$$

where

- $T_k$  = blackbody disk temperature of the planet, K
- $d$  = planet diameter, km
- $R$  = distance to planet, km
- $\theta$  = angular distance from planet center to antenna beam center
- $\theta_0$  = antenna half-power beamwidth (full beamwidth at half power)
- $G$  = antenna gain ratio  $\left[ 10^{(G(\text{dBi})/10)} \right]$  including atmospheric attenuation.

An alternative method for calculating the noise contribution for a planetary disk somewhat smaller than the antenna beamwidth is presented in JPL document D-33697 (*System Noise Temperature Increase from the Sun, Moon, or Planet Blackbody Disk Temperature*, by Anil Kantak and Stephen Slobin, December 1, 2005). Figure 20 shows an excerpt from that document (Figure 8), that indicates the percentage of total antenna power on a planetary disk, for ratios of half-power beamwidth to disk angular diameter in the range 2.0 to 5.0. For other half-power beamwidth/diameter ratios, that document should be consulted.

For a particular case (Venus on February 1, 2006, as seen from the DSS-13 34-m beam waveguide antenna at X-band), the following calculation is made:

$$\text{planet diameter } (d) = 12,104 \text{ km}$$

$$\text{planet disk temperature } (T_k) = 625 \text{ K at X-band (Table 20)}$$

range from earth ( $R$ ) = 0.318 AU = 47,572,800 km

$$\text{disk angular diameter} \left( \tan^{-1} \left[ \frac{d}{R} \right] \right) = 0.0146 \text{ degrees}$$

half-power beamwidth ( $\theta_0$ ) = 0.066 degrees

beamwidth/diameter = 4.521

power ratio from Figure 20 = 0.041

antenna efficiency ( $\eta$ ) = 0.673 without atmospheric loss at 39 deg. elevation

= 0.663 with clear sky atmospheric loss at 39 deg. elevation

The noise temperature calculated for the Figure 20 example is

$$T_{venus} = 625 \times 0.041 \times 0.663 = 16.99 \text{ K}$$

Using Equation 15 above, the numerical gain of the DSS-13 antenna is first calculated using an efficiency of 0.663 (includes clear sky atmosphere loss),

$$G = \eta \left( \frac{\pi D}{\lambda} \right)^2 = 5,966,230 \quad (16)$$

where

$D$  = antenna diameter = 34 m

$\lambda$  = wavelength = 0.0356 m at 8420 MHz (X-band)

therefore

$$T_{venus} = \left( \frac{625 \times 5,966,230 \times 12,104^2}{16 \times 47,572,800^2} \right) = 15.09 \text{ K}$$

The measured noise temperature increase from Venus was 16.18 K, so Equation (15) gives an estimate about 6.7% low, and the Figure 20 method gives an estimate about 5.0% high.

Table 20 presents all the parameters needed for calculation of planetary noise contributions. Also given are the maximum values of expected X-band and Ka-band noise contributions for the mean minimum distance from Earth, with the antenna beam pointed at the center of the planet ( $\theta=0$ ). Corresponding S-band noise temperature increases will be approximately 1/13 as large as the X-band increases because of the lower antenna gain (wider beamwidth) at the lower frequency.

In the case of Jupiter, there is a significant and variable non-thermal component of the noise temperature. Thus the effective blackbody disk temperature at S-band appears to be much higher than at X-band. The S-band noise temperature increase will be approximately 1/6

the X-band values for average Jupiter emission; it will be about 1/3 the X-band values for maximum Jupiter emission. Except for Venus and Jupiter at inferior conjunction (minimum distance), the noise contribution from the planets at S-band is negligible.

The expression (Equation 15) for  $T_{pl}$  assumes that the angular extent of the radiating source is small compared to the antenna beamwidth. This approximation is adequate at X-band except for Venus near inferior conjunction (apparent diameter = 0.018 deg) using a 70-m antenna at X-band (beamwidth = 0.032 deg). At Ka-band with a 34-m antenna (beamwidth = 0.0174 deg), the approximation is not adequate for Venus near inferior conjunction and may not be adequate for Mars near inferior conjunction (apparent diameter = 0.005 deg). The expression also assumes that the antenna main beam has a Gaussian shape, with circular symmetry. Antenna gains and half-power beamwidths are given in modules 101, 102, 103, and 104.

#### 2.4.4 *Galactic Noise*

The center of the Milky Way galaxy is located near -30 degrees declination, 17 h 40 min right ascension. It is possible for a spacecraft with a declination of -30 deg to be in the vicinity of the galactic center, and an increase of system noise temperature would then be observed. A declination of -30 degrees is not typically achieved by spacecraft moving in the plane of the ecliptic, but there are some circumstances (for example, a flight out of the ecliptic) where this location may be observed. Galactic noise temperature contributions at frequencies above 10 GHz are typically insignificant. At S-band, looking directly at the galactic center, a noise temperature increase of about 10 K would be observed. A map of the galactic noise distribution can be seen in chapter 8 of the classic reference J. D. Kraus, *Radio Astronomy*, Cygnus-Quasar Books, Powell, Ohio, 1986.

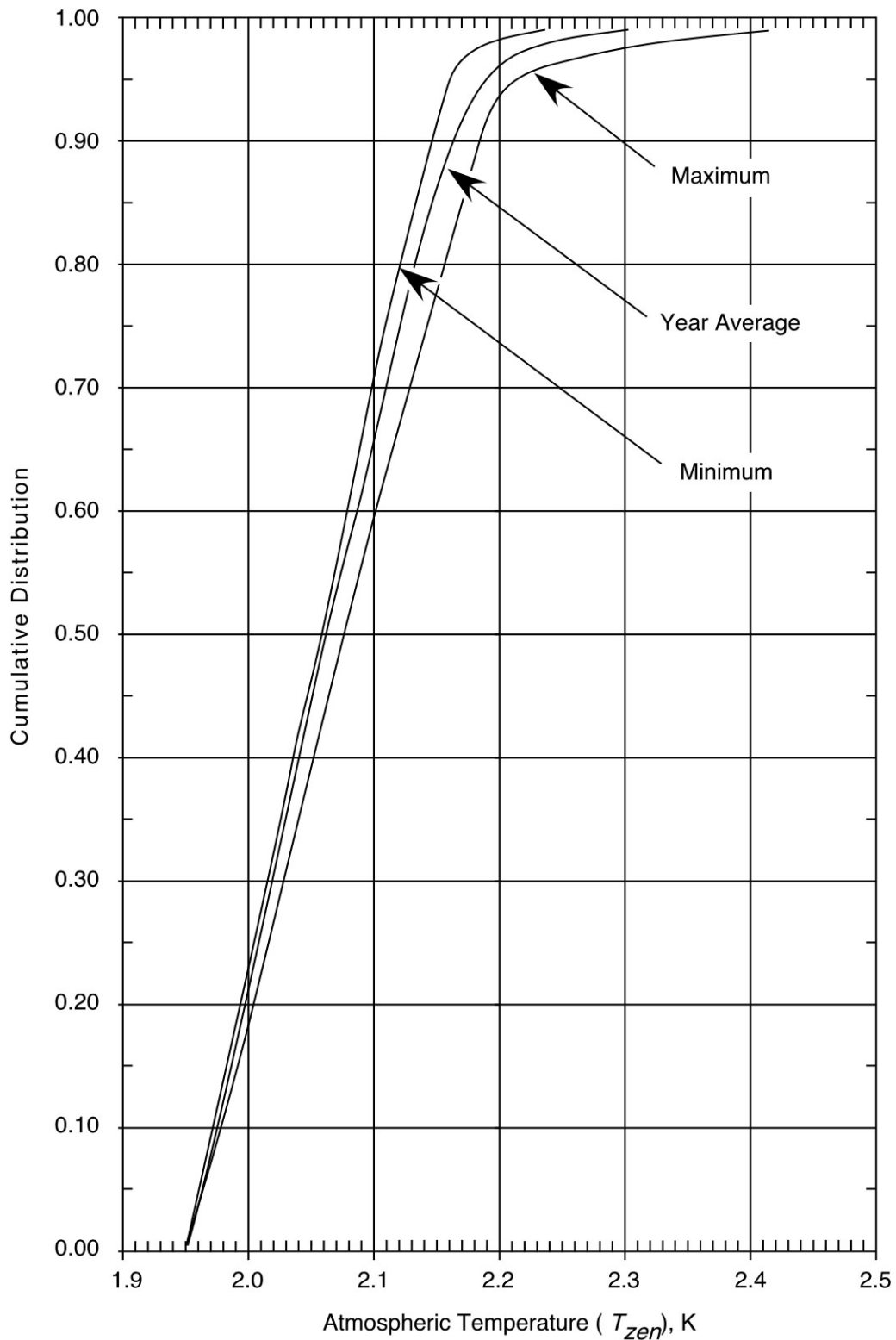


Figure 1. Cumulative Distributions of Zenith Atmospheric Noise Temperature at L-Band and S-Band, Goldstone DSCL

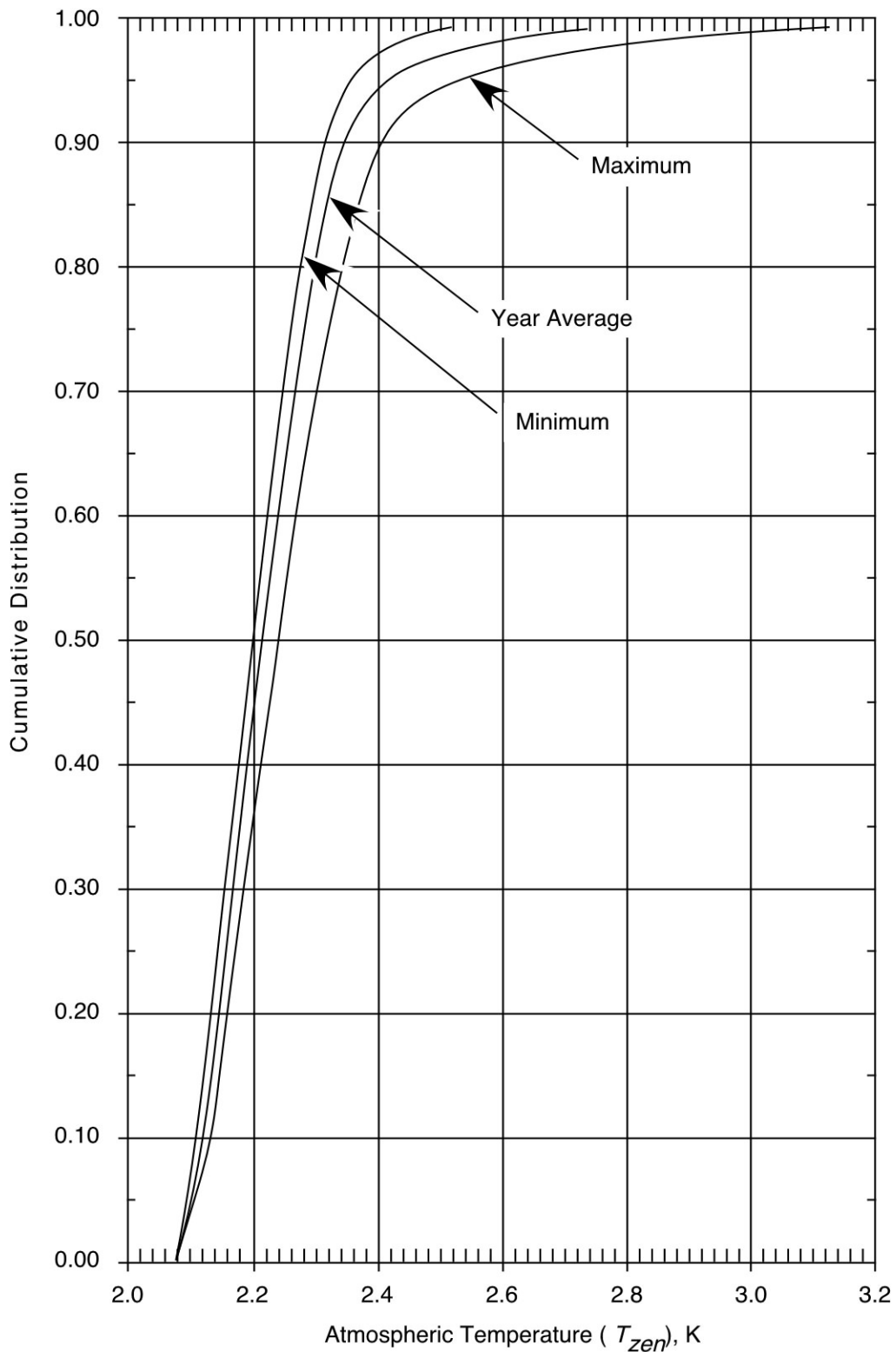


Figure 2. Cumulative Distributions of Zenith Atmospheric Noise Temperature at L-Band and S-Band, Canberra DSCL

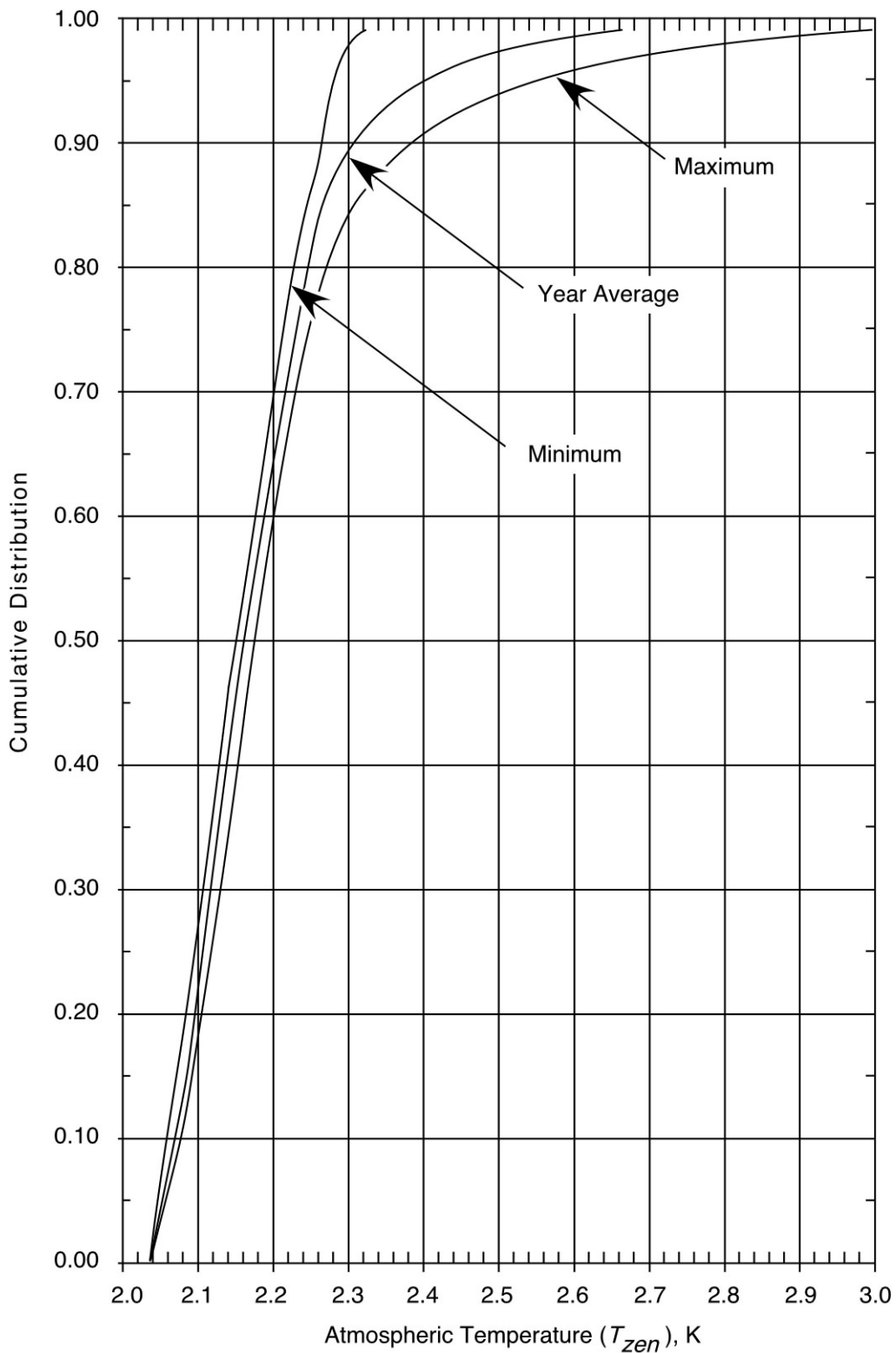


Figure 3. Cumulative Distributions of Zenith Atmospheric Noise Temperature at L-Band and S-Band, Madrid DSCC

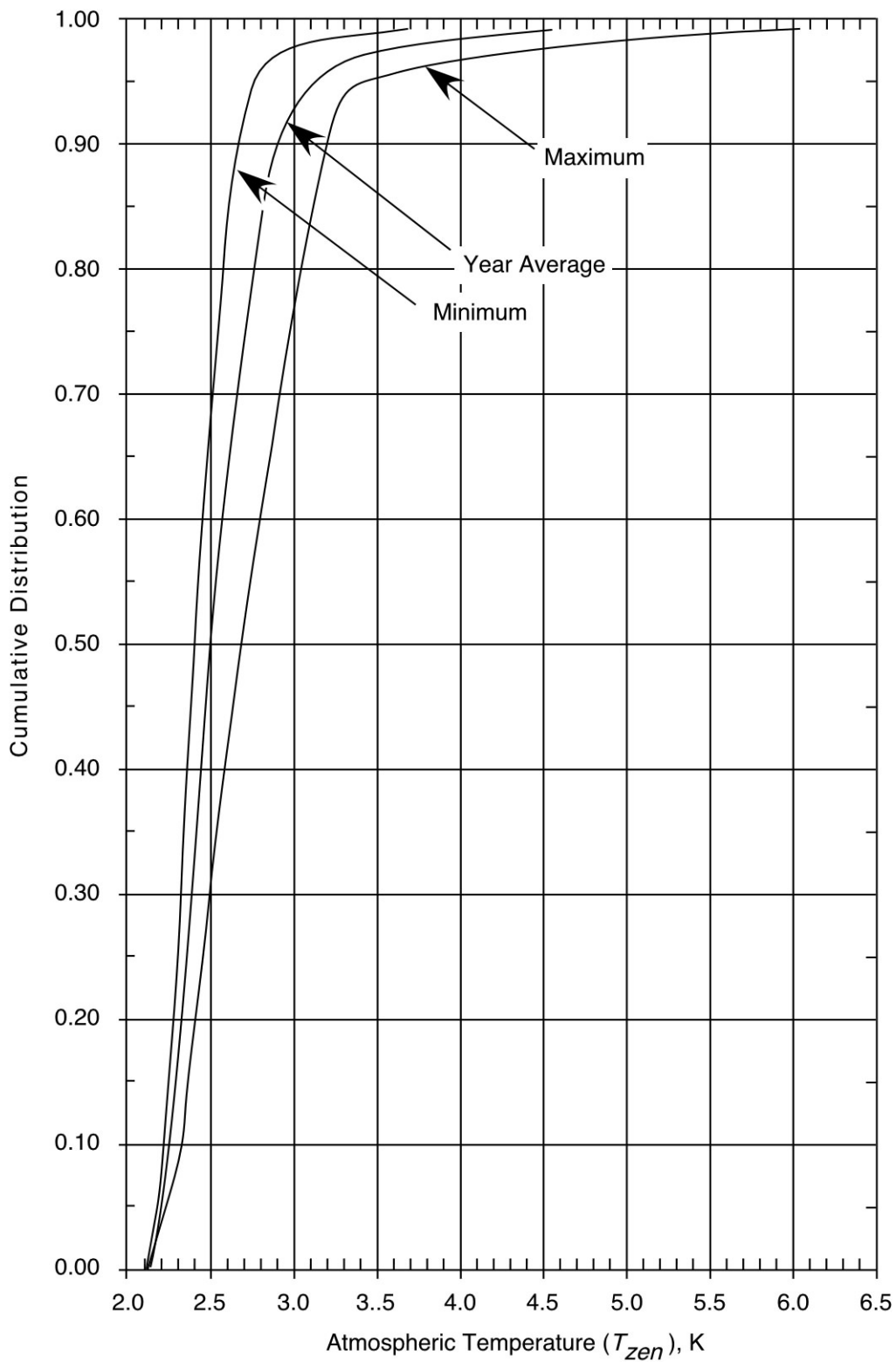


Figure 4. Cumulative Distributions of Zenith Atmospheric Noise Temperature at X-Band, Goldstone DSCC

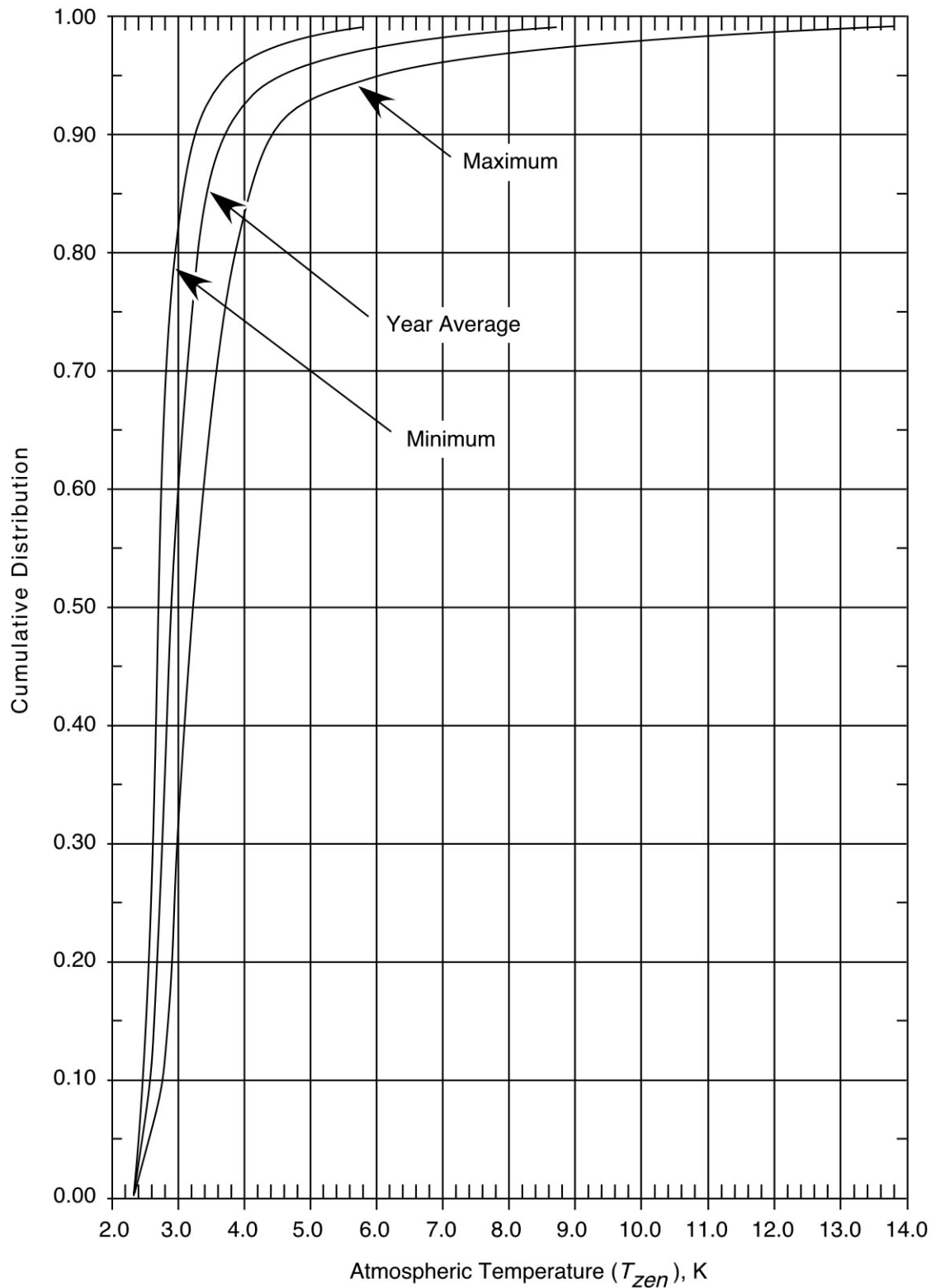


Figure 5. Cumulative Distributions of Zenith Atmospheric Noise Temperature at X-Band, Canberra DSCC

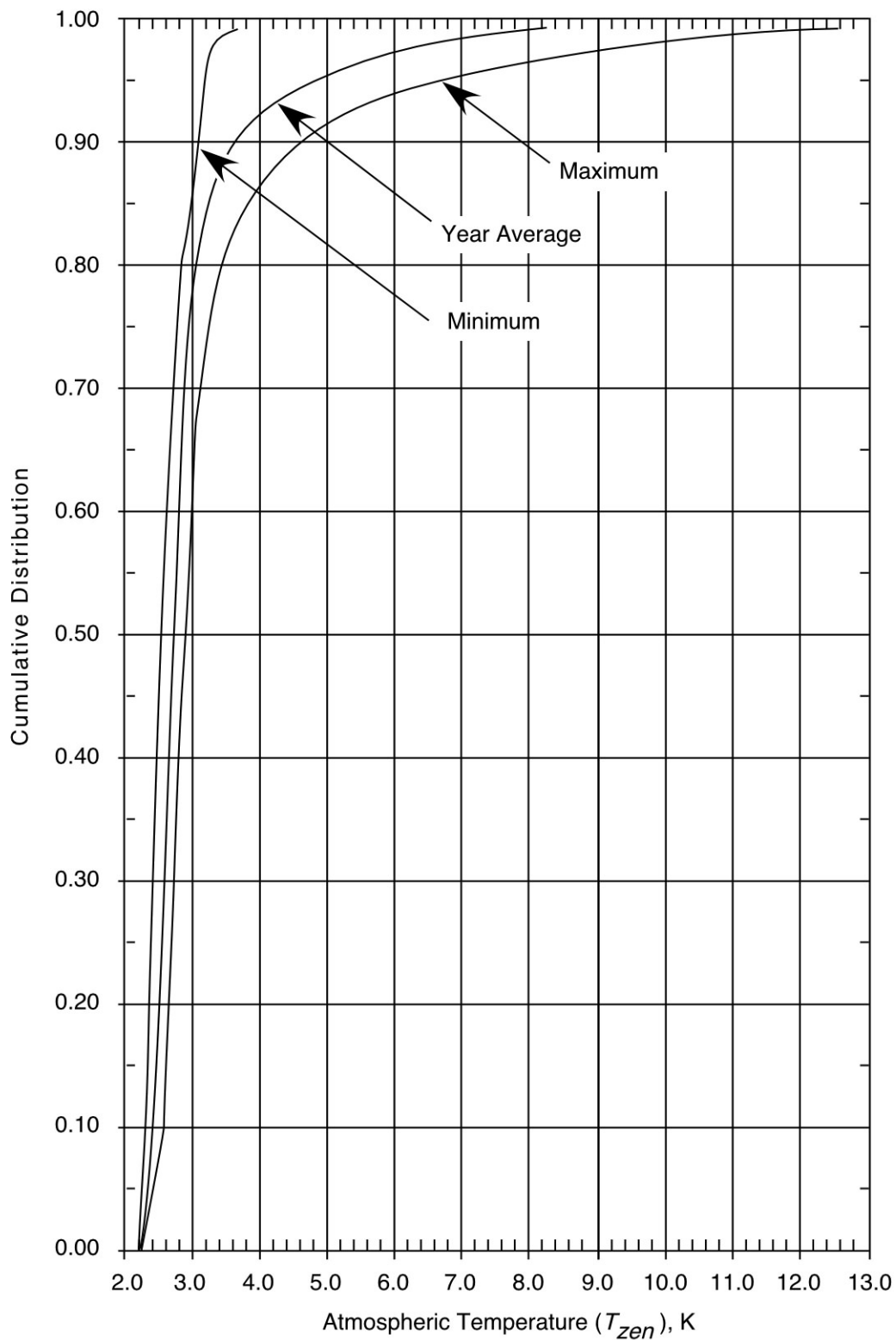


Figure 6. Cumulative Distributions of Zenith Atmospheric Noise Temperature at X-Band, Madrid DSCL

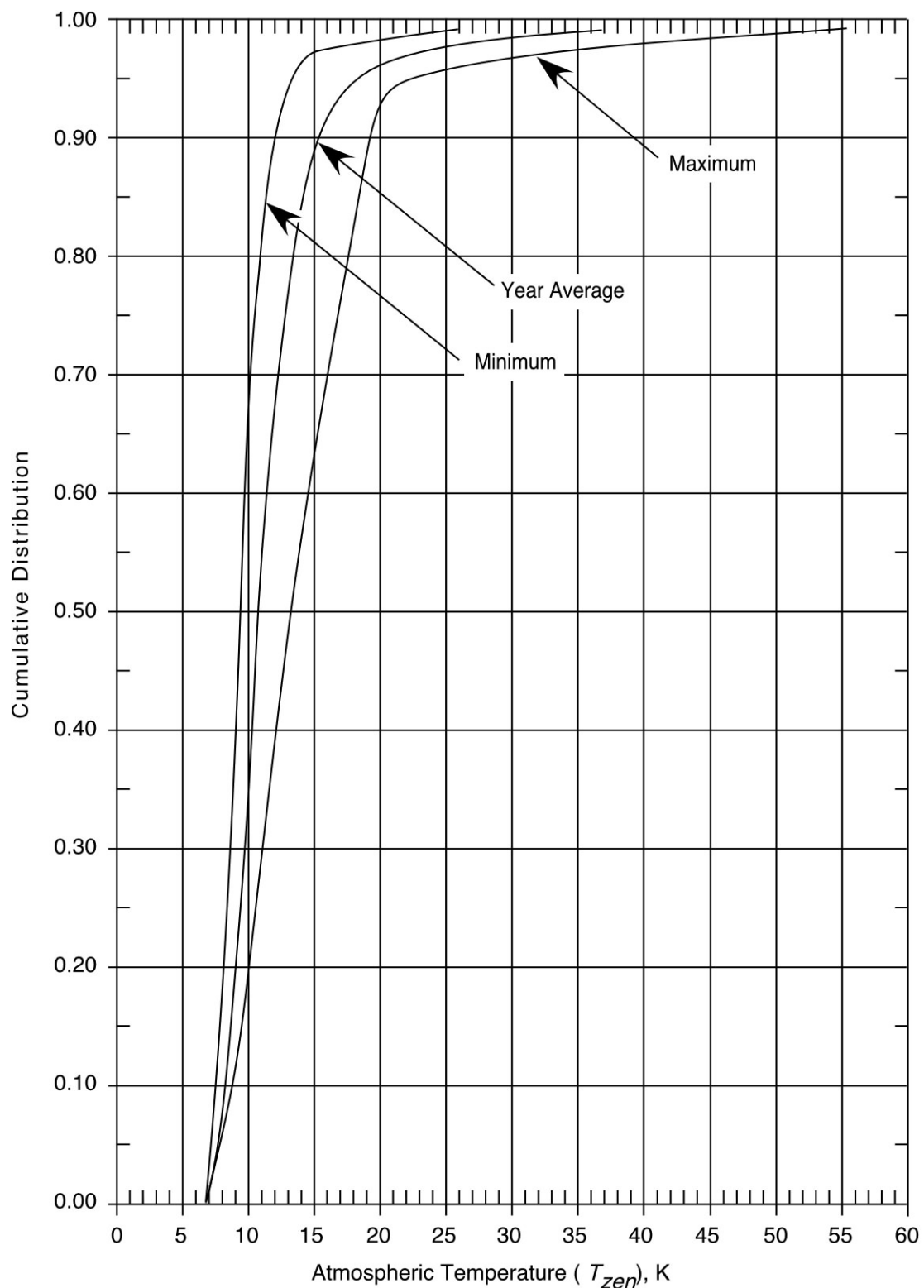


Figure 7. Cumulative Distributions of Zenith Atmospheric Noise Temperature at Ka-Band, Goldstone DSCC

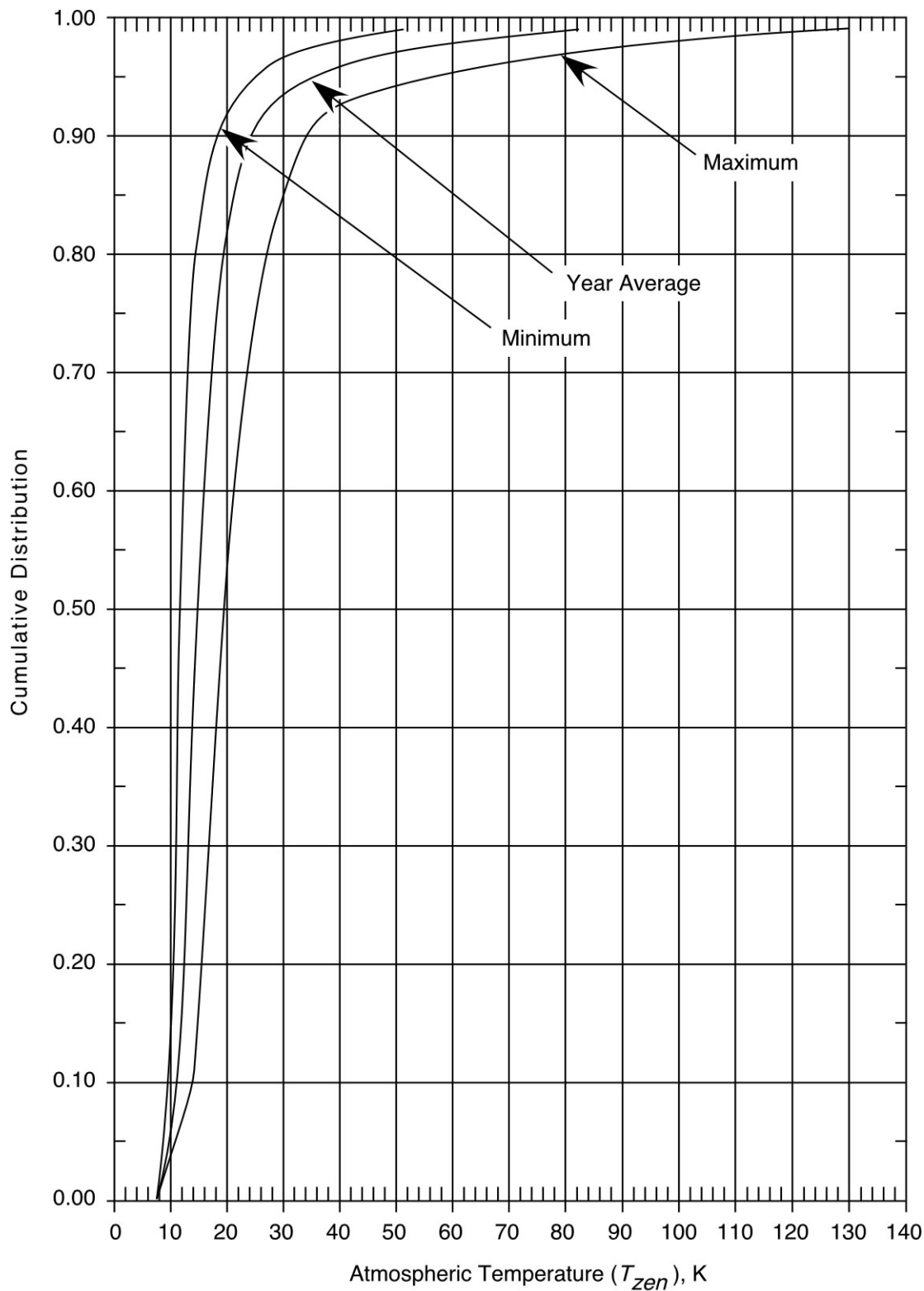


Figure 8. Cumulative Distributions of Zenith Atmospheric Noise Temperature at Ka-Band, Canberra DSCL

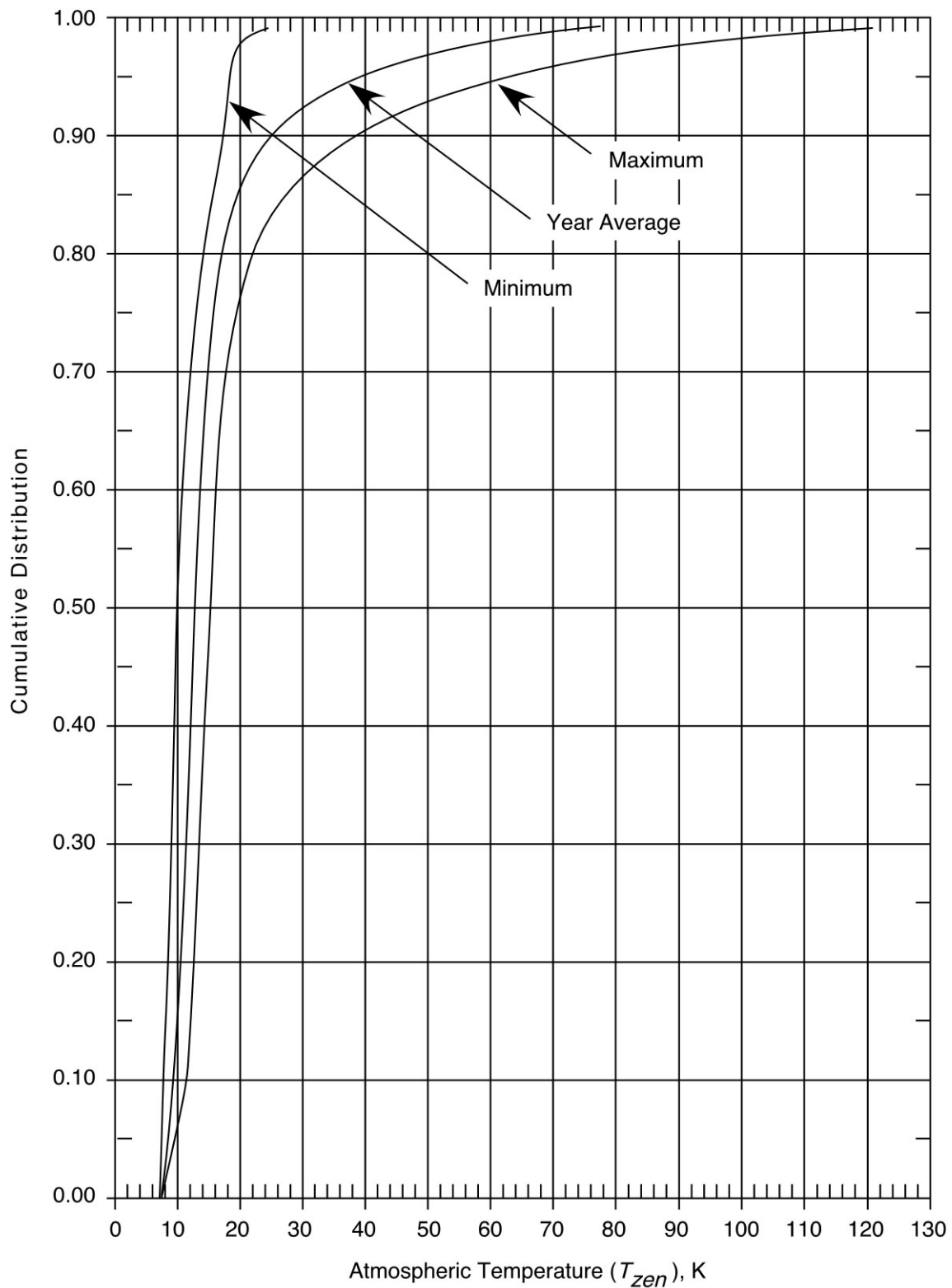


Figure 9. Cumulative Distributions of Zenith Atmospheric Noise Temperature at Ka-Band, Madrid DSCC

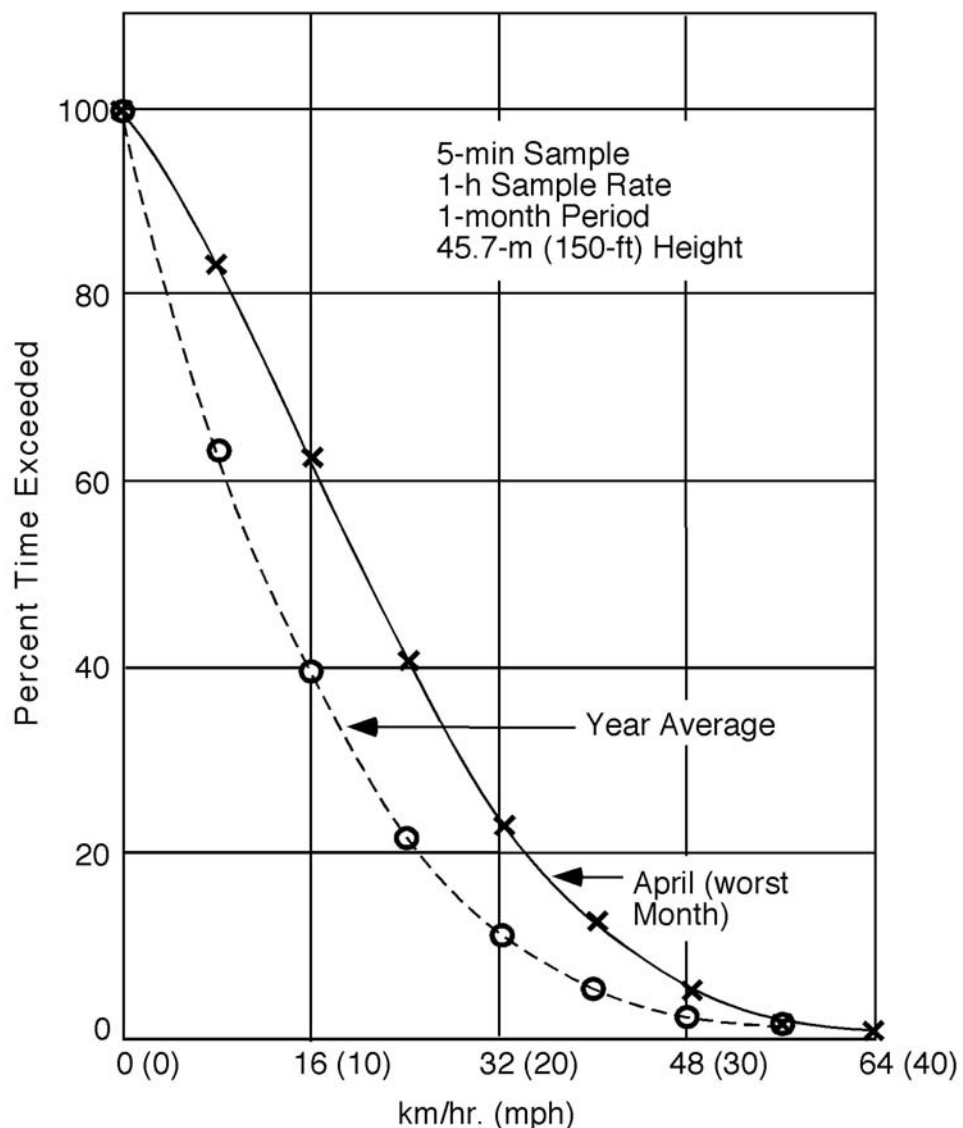


Figure 10. Probability Distribution of Wind Conditions at Goldstone

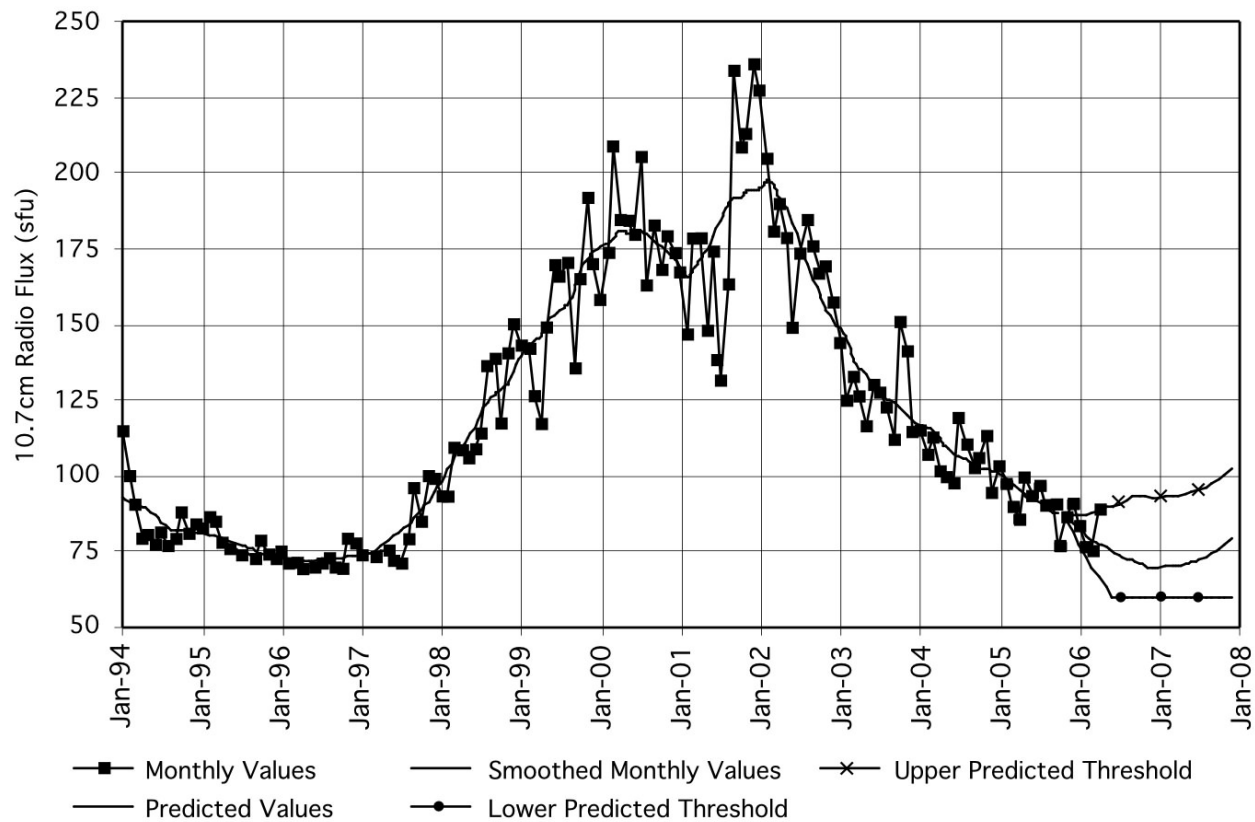


Figure 11. Solar Radio Flux at 2800 MHz (10.7 cm wavelength) During Solar Cycle 23 (1996–2007)

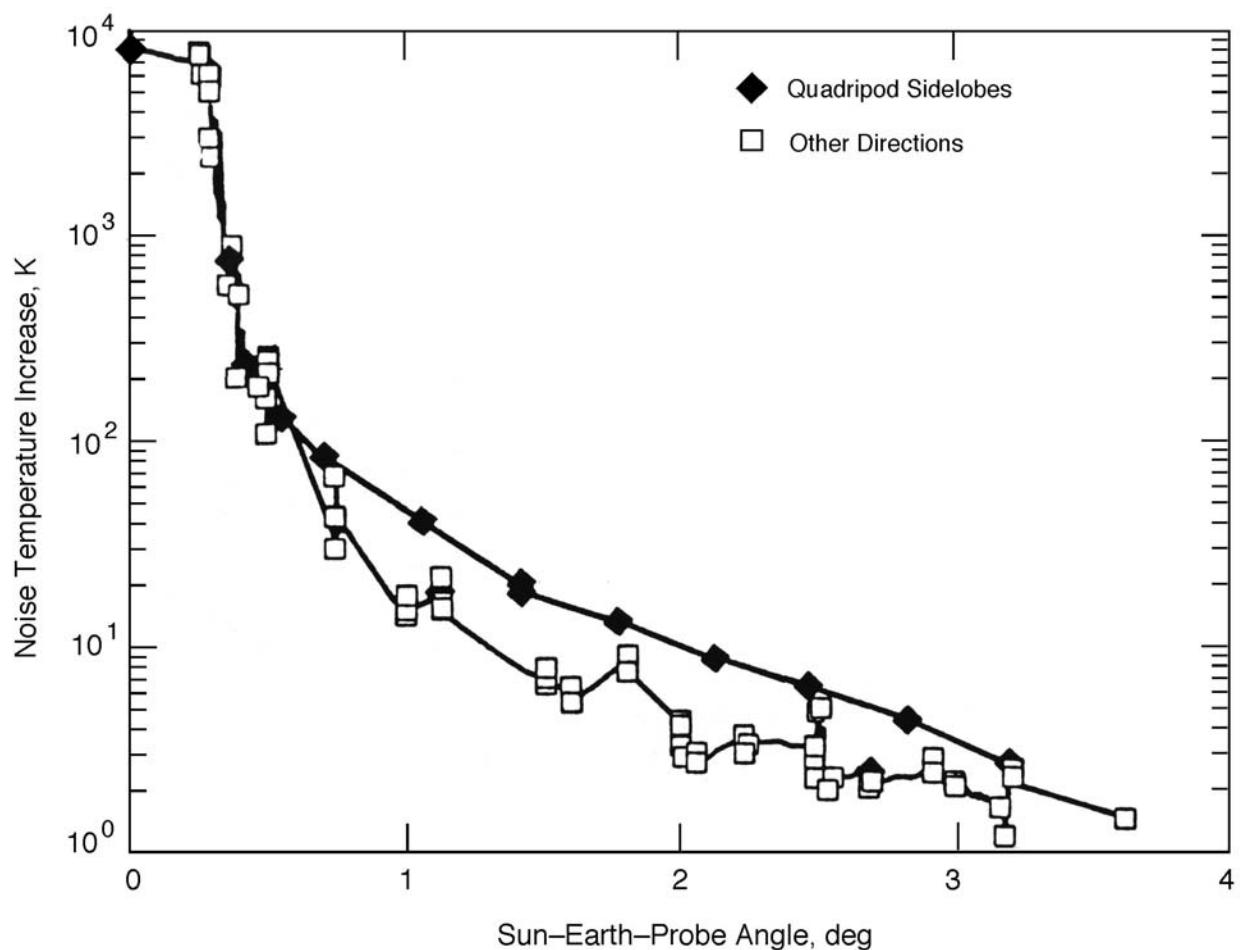
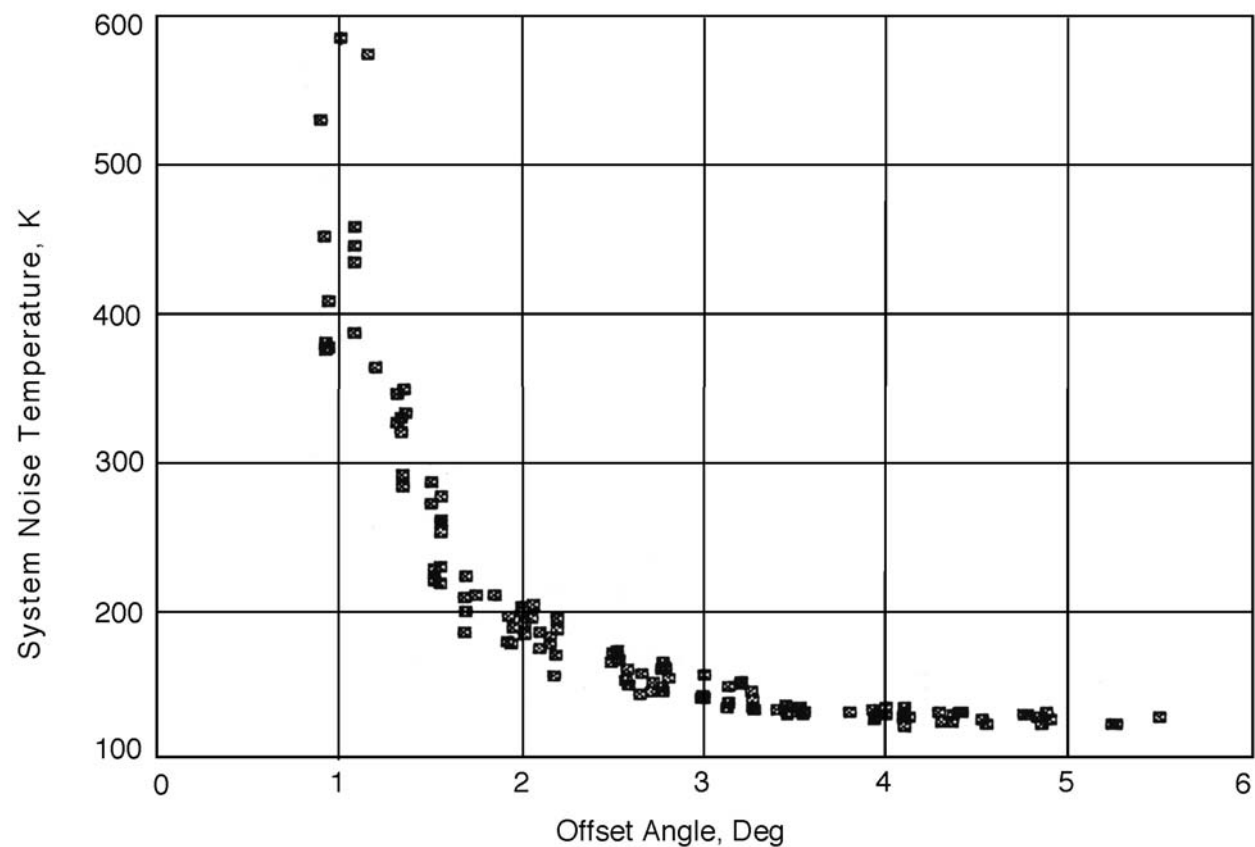


Figure 12. DSS-15 HEF Antenna X-Band System Noise Temperature Increases Due to the Sun at Various Offset Angles, Showing Larger Increases Perpendicular to Quadripod Directions



810-005, Rev. E  
105, Rev. B

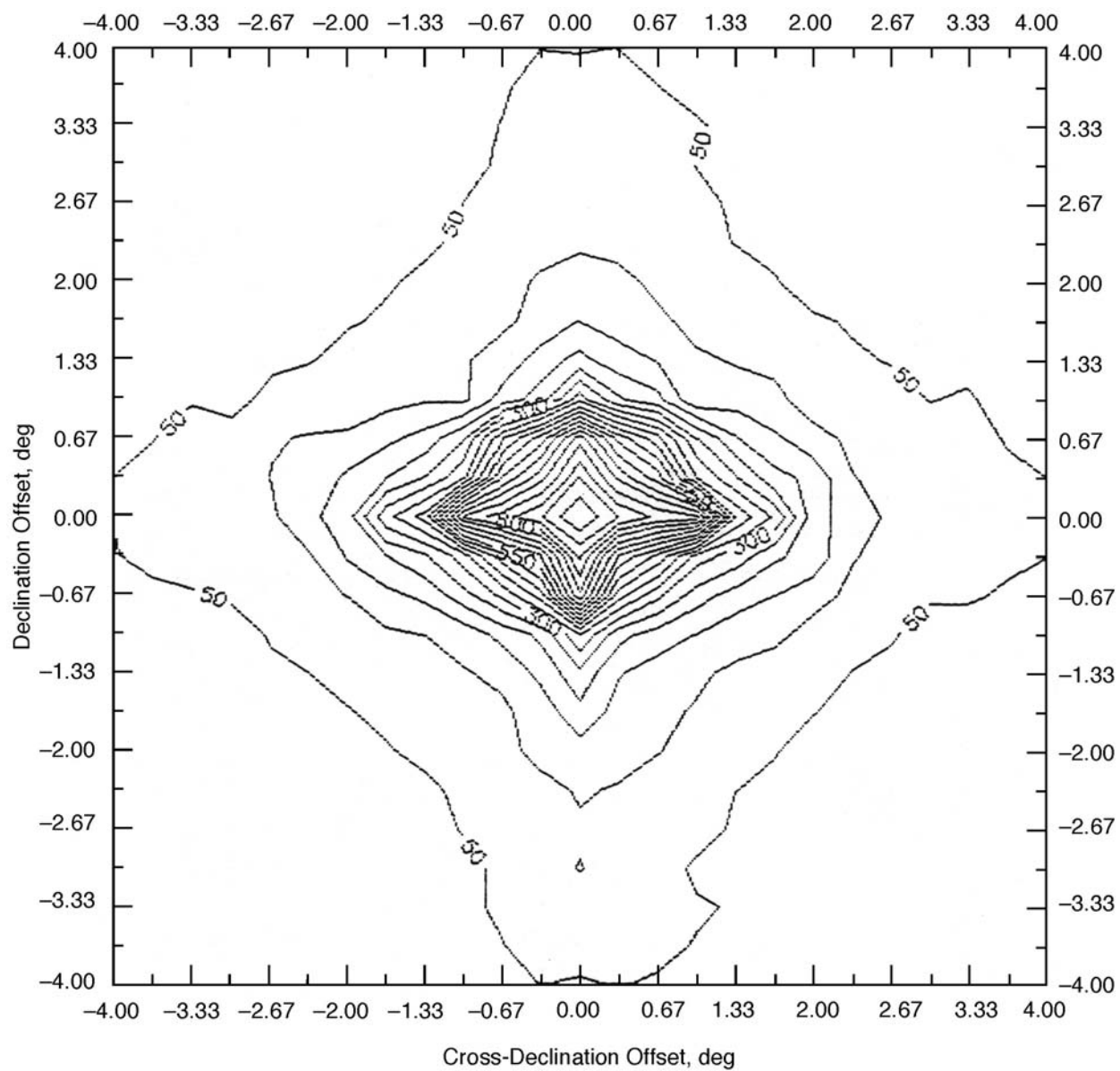


Figure 14. DSS-12 S-Band Total System Noise Temperature at Various Declination and Cross-Declination Offsets from the Sun

810-005, Rev. E  
105, Rev. B

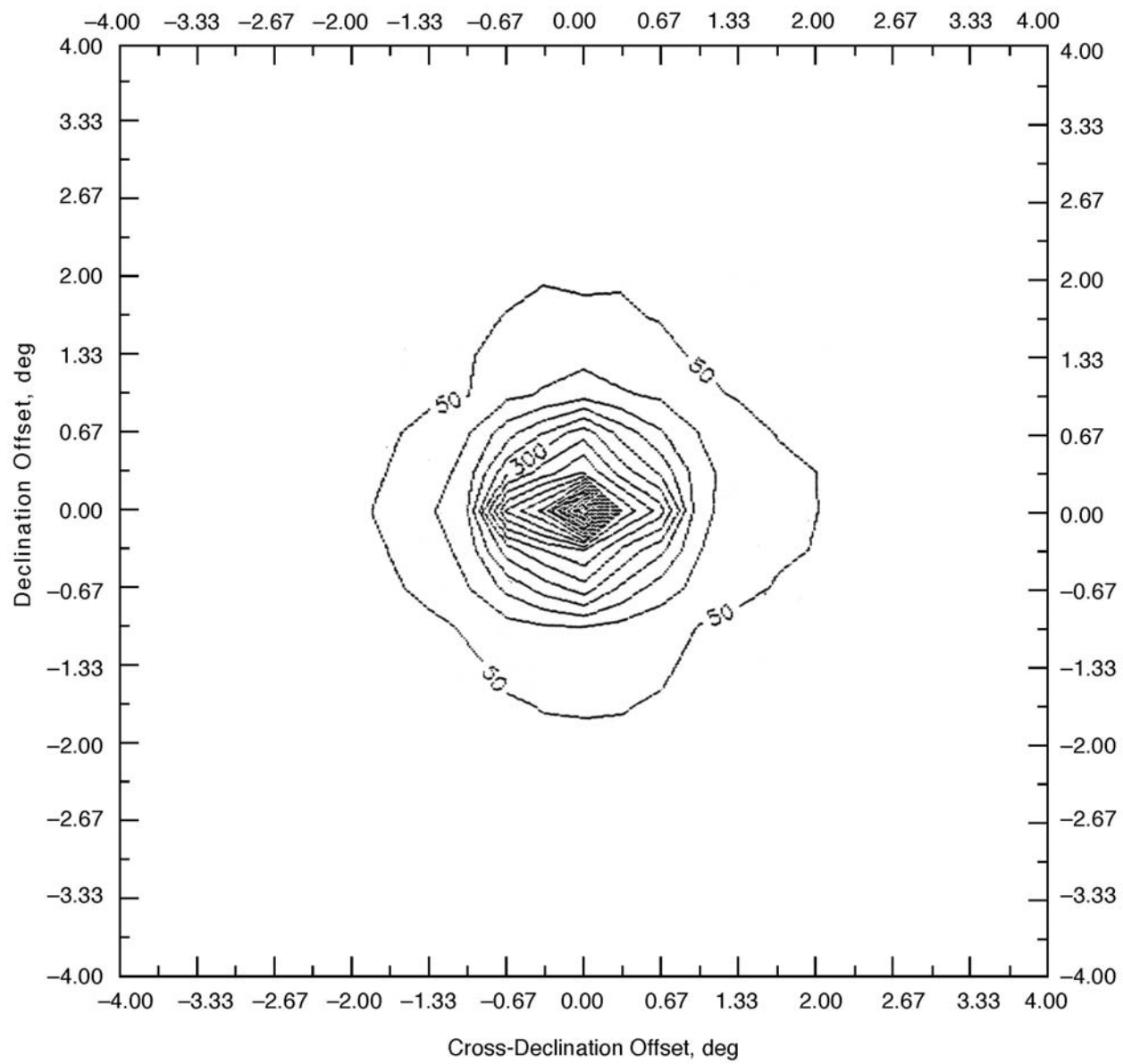


Figure 15. DSS-12 X-Band Total System Noise Temperature at Various Declination and Cross-Declination Offsets from the Sun

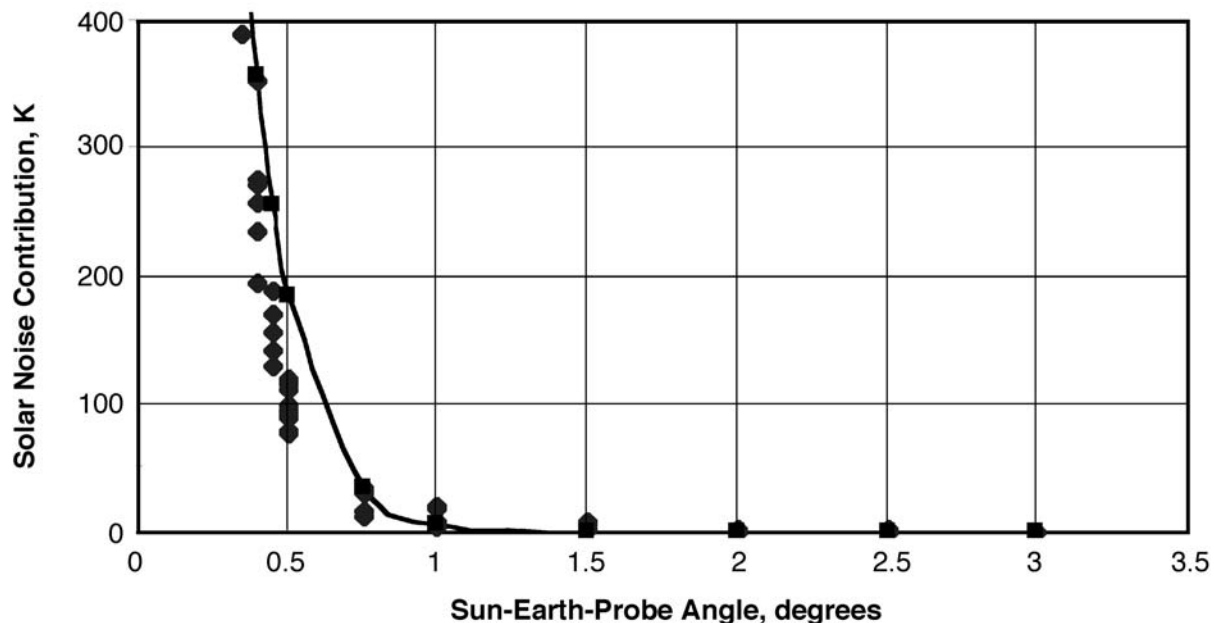


Figure 16. DSS-13 Beam-Waveguide Antenna X-Band Noise Temperature Increase Versus Offset Angle, March 1996

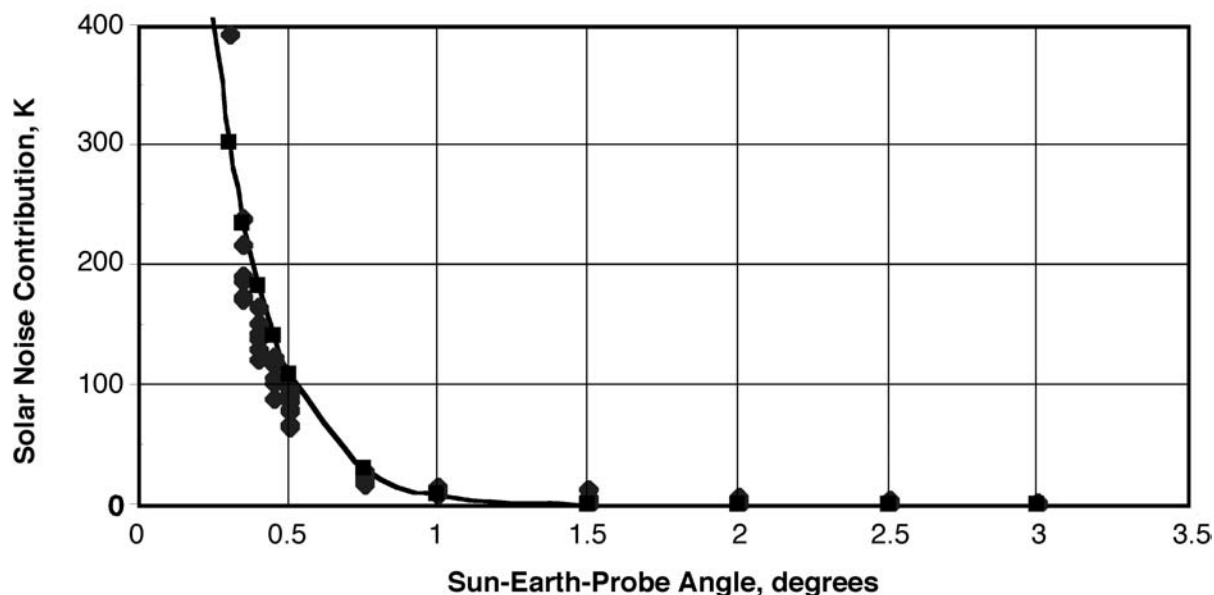


Figure 17. DSS-13 Beam-Waveguide Antenna Ka-Band Noise Temperature Increase Versus Offset Angle, March 1996

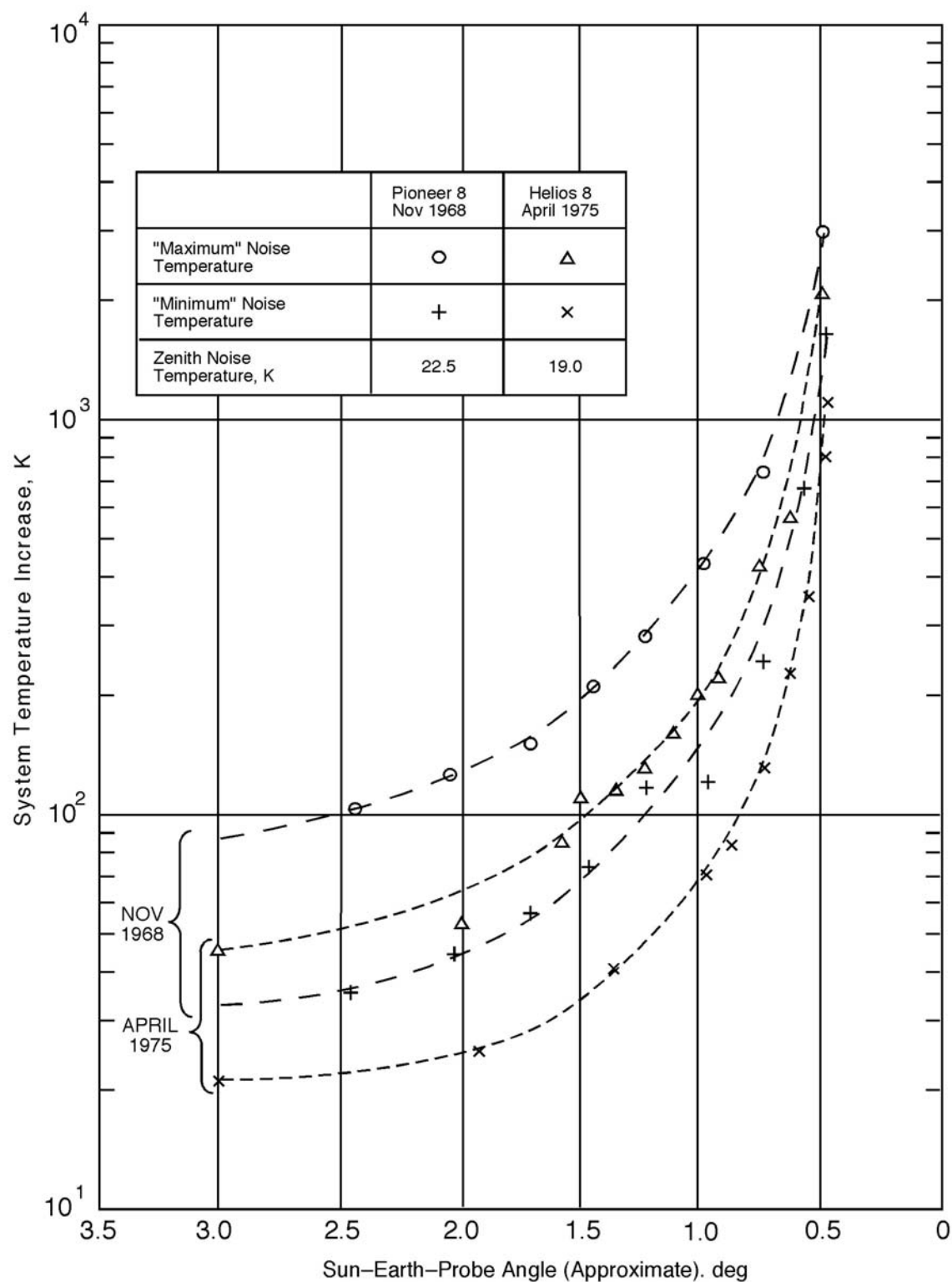


Figure 18. Total S-Band System Noise Temperature for 70-m Antennas Tracking Spacecraft Near the Sun (Derived from 64-m Measurements)

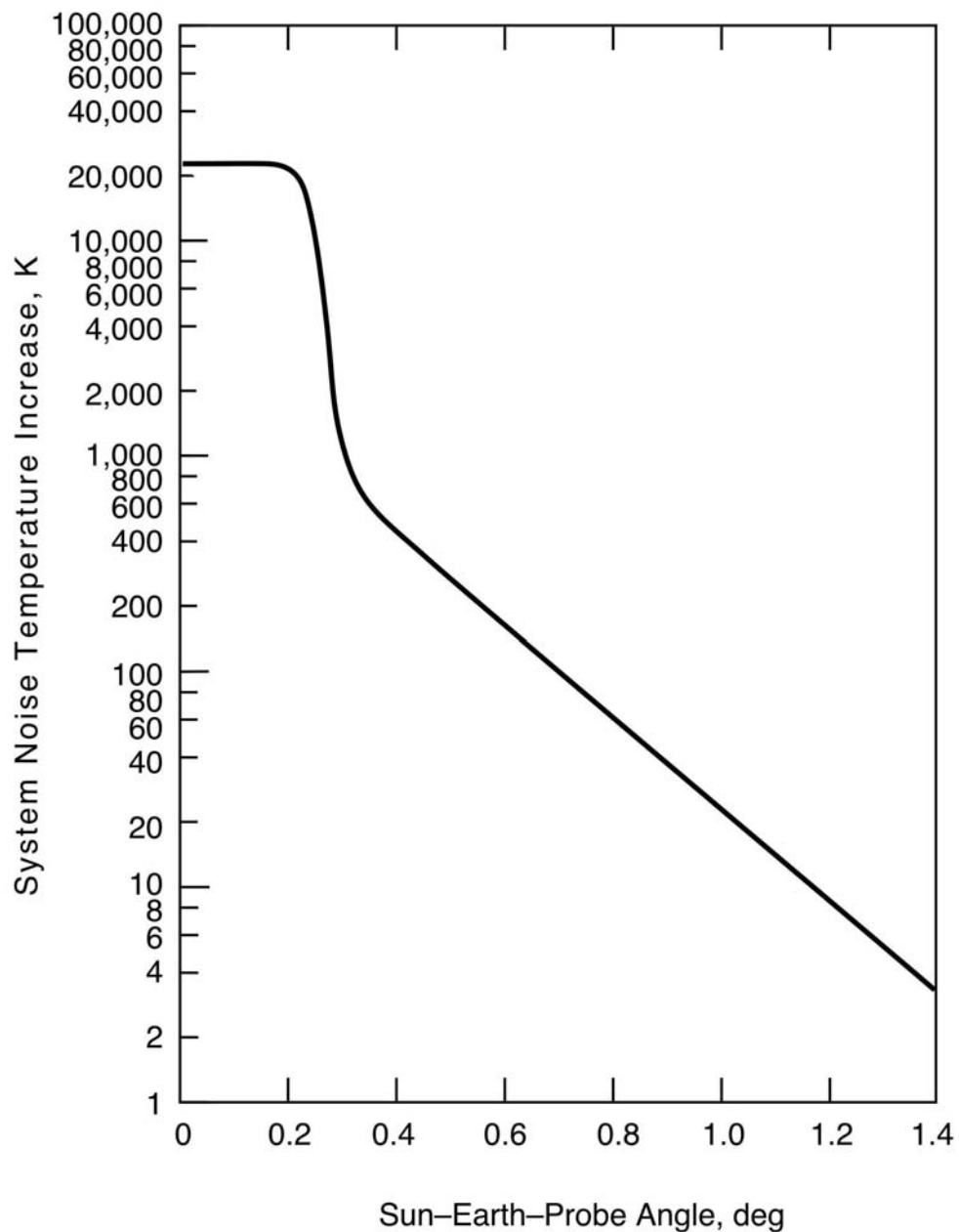


Figure 19. X-Band Noise Temperature Increase for 70-m Antennas as a Function of Sun-Earth-Probe Angle, Nominal Sun, 23,000 K Disk Temperature

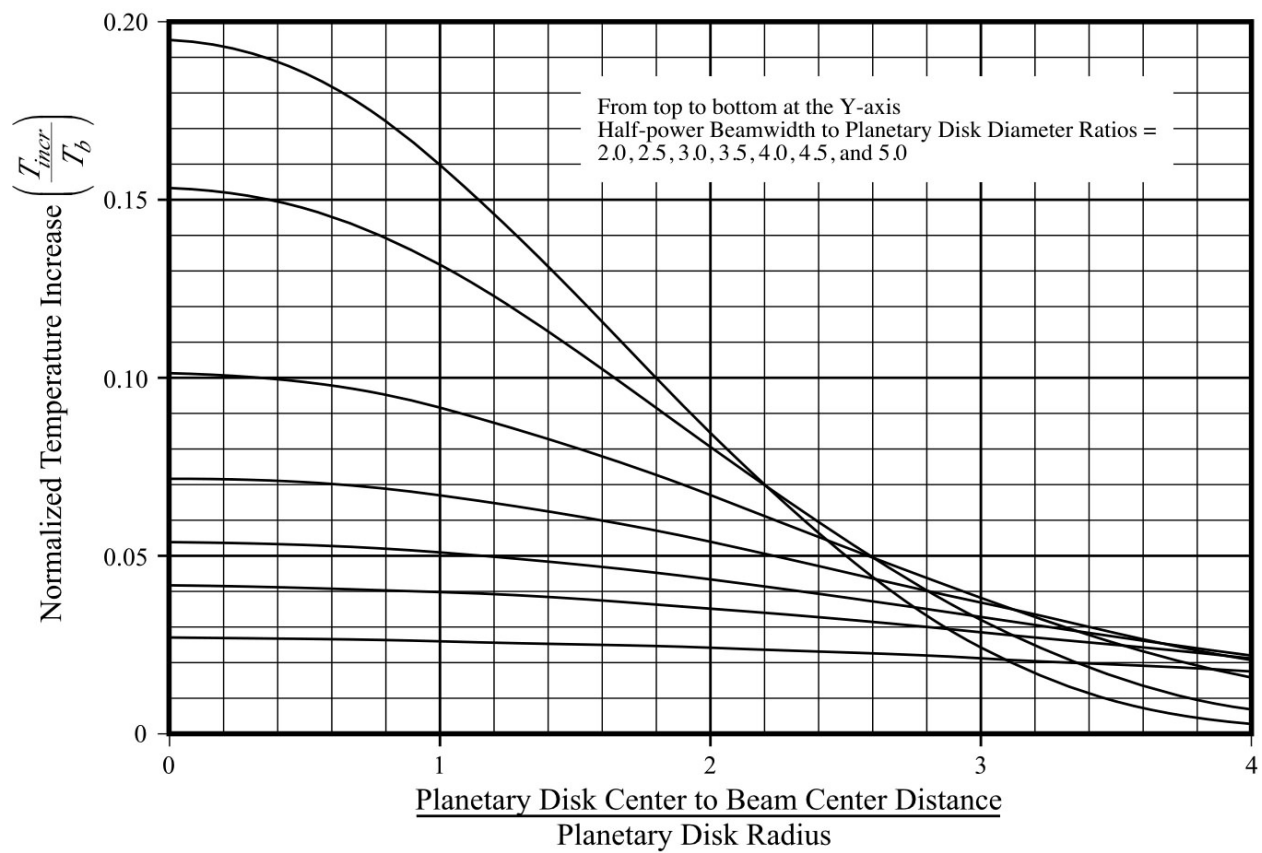


Figure 20. Normalized Temperature Increase for Half-power Beamwidth to Planetary Disk Diameter Ratios from 2.0 to 5.0

Table 1. Cumulative Distributions of Zenith Atmospheric Noise Temperature at L- and S-Bands for Goldstone DSCL, K

CD	January	February	March	April	May	June
0.00	1.948	1.948	1.948	1.948	1.948	1.948
0.10	1.972	1.971	1.972	1.973	1.975	1.976
0.20	1.994	1.992	1.994	1.995	1.997	1.998
0.25	2.004	2.003	2.004	2.005	2.008	2.008
0.30	2.014	2.013	2.015	2.015	2.018	2.019
0.40	2.035	2.034	2.035	2.036	2.039	2.041
0.50	2.056	2.056	2.056	2.056	2.060	2.063
0.60	2.077	2.077	2.077	2.077	2.082	2.086
0.70	2.100	2.099	2.098	2.099	2.105	2.110
0.80	2.125	2.124	2.120	2.120	2.129	2.136
0.85	2.140	2.138	2.132	2.132	2.142	2.149
0.90	2.158	2.158	2.145	2.144	2.158	2.164
0.92	2.169	2.172	2.152	2.150	2.165	2.170
0.93	2.178	2.182	2.156	2.153	2.170	2.174
0.94	2.188	2.195	2.160	2.156	2.175	2.178
0.95	2.204	2.212	2.165	2.160	2.182	2.183
0.96	2.222	2.233	2.173	2.166	2.190	2.191
0.97	2.249	2.266	2.187	2.174	2.204	2.202
0.98	2.294	2.316	2.209	2.190	2.235	2.227
0.99	2.393	2.413	2.268	2.237	2.275	2.285

Table 1 (Cont'd). Cumulative Distributions of Zenith Atmospheric Noise Temperature at L- and S-Bands for Goldstone DSCL, K

CD	July	August	September	October	November	December	Minimum	Year Average	Maximum
0.00	1.948	1.948	1.948	1.948	1.948	1.948	1.948	1.948	1.948
0.10	1.978	1.978	1.978	1.975	1.972	1.972	1.971	1.974	1.978
0.20	2.003	2.003	2.000	1.998	1.994	1.993	1.992	1.997	2.003
0.25	2.014	2.014	2.011	2.009	2.004	2.004	2.003	2.007	2.014
0.30	2.026	2.026	2.021	2.019	2.015	2.014	2.013	2.018	2.026
0.40	2.049	2.051	2.044	2.040	2.036	2.035	2.034	2.040	2.051
0.50	2.073	2.076	2.067	2.062	2.058	2.056	2.056	2.062	2.076
0.60	2.100	2.101	2.091	2.083	2.081	2.077	2.077	2.084	2.101
0.70	2.128	2.127	2.118	2.105	2.103	2.100	2.098	2.108	2.128
0.80	2.155	2.152	2.147	2.129	2.129	2.124	2.120	2.133	2.155
0.85	2.169	2.167	2.161	2.142	2.143	2.138	2.132	2.146	2.169
0.90	2.183	2.183	2.177	2.157	2.159	2.154	2.144	2.162	2.183
0.92	2.190	2.190	2.185	2.164	2.167	2.162	2.150	2.170	2.190
0.93	2.194	2.194	2.188	2.168	2.171	2.167	2.153	2.175	2.194
0.94	2.199	2.199	2.193	2.173	2.176	2.174	2.156	2.180	2.199
0.95	2.204	2.203	2.197	2.178	2.180	2.184	2.160	2.188	2.212
0.96	2.211	2.210	2.203	2.184	2.188	2.200	2.166	2.197	2.233
0.97	2.220	2.219	2.211	2.193	2.205	2.221	2.174	2.212	2.266
0.98	2.238	2.238	2.230	2.216	2.238	2.258	2.190	2.240	2.316
0.99	2.280	2.254	2.286	2.273	2.313	2.351	2.237	2.302	2.413

Table 2. Cumulative Distributions of Zenith Atmospheric Noise Temperature at L- and S-Bands for Canberra DSCC, K

CD	January	February	March	April	May	June
0.00	2.076	2.076	2.076	2.076	2.076	2.076
0.10	2.119	2.130	2.123	2.118	2.112	2.109
0.20	2.146	2.158	2.150	2.144	2.136	2.132
0.25	2.159	2.172	2.162	2.156	2.148	2.144
0.30	2.172	2.186	2.175	2.167	2.159	2.155
0.40	2.197	2.213	2.200	2.191	2.182	2.178
0.50	2.223	2.240	2.227	2.216	2.205	2.202
0.60	2.250	2.269	2.254	2.242	2.228	2.227
0.70	2.278	2.301	2.282	2.268	2.254	2.254
0.80	2.311	2.342	2.315	2.297	2.284	2.283
0.85	2.330	2.368	2.335	2.314	2.304	2.299
0.90	2.356	2.404	2.361	2.339	2.333	2.323
0.92	2.369	2.430	2.373	2.356	2.351	2.340
0.93	2.377	2.455	2.381	2.367	2.362	2.353
0.94	2.389	2.490	2.391	2.384	2.375	2.367
0.95	2.405	2.537	2.408	2.404	2.393	2.391
0.96	2.428	2.609	2.432	2.426	2.417	2.428
0.97	2.464	2.692	2.471	2.464	2.452	2.481
0.98	2.540	2.830	2.532	2.537	2.517	2.546
0.99	2.698	3.131	2.689	2.645	2.633	2.648

Table 2 (Cont'd). Cumulative Distributions of Zenith Atmospheric Noise Temperature at L- and S-Bands for Canberra DSCC, K

CD	July	August	September	October	November	December	Minimum	Year Average	Maximum
0.00	2.076	2.076	2.076	2.076	2.076	2.076	2.076	2.076	2.076
0.10	2.108	2.108	2.110	2.112	2.118	2.117	2.108	2.115	2.130
0.20	2.131	2.131	2.134	2.137	2.143	2.143	2.131	2.140	2.158
0.25	2.143	2.143	2.146	2.149	2.156	2.156	2.143	2.153	2.172
0.30	2.154	2.154	2.158	2.161	2.168	2.169	2.154	2.165	2.186
0.40	2.176	2.176	2.181	2.184	2.193	2.195	2.176	2.189	2.213
0.50	2.199	2.199	2.205	2.208	2.219	2.221	2.199	2.214	2.240
0.60	2.223	2.222	2.229	2.232	2.247	2.248	2.222	2.239	2.269
0.70	2.248	2.246	2.255	2.259	2.279	2.277	2.246	2.267	2.301
0.80	2.275	2.273	2.283	2.292	2.316	2.312	2.273	2.298	2.342
0.85	2.292	2.290	2.301	2.315	2.341	2.336	2.290	2.318	2.368
0.90	2.314	2.317	2.324	2.350	2.385	2.371	2.314	2.348	2.404
0.92	2.327	2.335	2.340	2.373	2.419	2.395	2.327	2.367	2.430
0.93	2.335	2.347	2.351	2.389	2.440	2.411	2.335	2.380	2.455
0.94	2.346	2.363	2.364	2.408	2.466	2.435	2.346	2.398	2.490
0.95	2.360	2.385	2.381	2.434	2.505	2.464	2.360	2.421	2.537
0.96	2.379	2.415	2.409	2.466	2.559	2.512	2.379	2.456	2.609
0.97	2.405	2.467	2.453	2.516	2.638	2.581	2.405	2.506	2.692
0.98	2.439	2.534	2.519	2.598	2.737	2.675	2.439	2.582	2.830
0.99	2.522	2.675	2.704	2.785	2.927	2.859	2.522	2.740	3.131

Table 3. Cumulative Distributions of Zenith Atmospheric Noise Temperature at L- and S-Bands for Madrid DSCC, K

CD	January	February	March	April	May	June
0.00	2.035	2.035	2.035	2.035	2.035	2.035
0.10	2.058	2.059	2.063	2.065	2.072	2.073
0.20	2.081	2.082	2.087	2.089	2.096	2.098
0.25	2.092	2.093	2.098	2.100	2.107	2.110
0.30	2.104	2.105	2.110	2.111	2.119	2.122
0.40	2.126	2.127	2.133	2.134	2.143	2.146
0.50	2.150	2.150	2.157	2.157	2.166	2.169
0.60	2.174	2.173	2.181	2.181	2.190	2.193
0.70	2.200	2.197	2.208	2.206	2.215	2.218
0.80	2.233	2.226	2.241	2.233	2.243	2.244
0.85	2.258	2.247	2.268	2.252	2.262	2.257
0.90	2.310	2.291	2.322	2.288	2.298	2.272
0.92	2.358	2.323	2.359	2.316	2.327	2.278
0.93	2.396	2.346	2.385	2.334	2.347	2.282
0.94	2.439	2.378	2.415	2.360	2.372	2.287
0.95	2.484	2.419	2.451	2.393	2.406	2.292
0.96	2.534	2.460	2.500	2.439	2.451	2.302
0.97	2.590	2.513	2.558	2.492	2.501	2.320
0.98	2.660	2.573	2.634	2.563	2.570	2.358
0.99	2.769	2.683	2.753	2.669	2.689	2.466

Table 3 (Cont'd). Cumulative Distributions of Zenith Atmospheric Noise Temperature at L- and S-Bands for Madrid DSCC, K

CD	July	August	September	October	November	December	Minimum	Year Average	Maximum
0.00	2.035	2.035	2.035	2.035	2.035	2.035	2.035	2.035	2.035
0.10	2.075	2.078	2.074	2.071	2.063	2.062	2.058	2.068	2.078
0.20	2.100	2.103	2.099	2.097	2.087	2.086	2.081	2.092	2.103
0.25	2.112	2.115	2.111	2.110	2.099	2.097	2.092	2.104	2.115
0.30	2.123	2.127	2.123	2.122	2.110	2.109	2.104	2.115	2.127
0.40	2.146	2.151	2.147	2.146	2.133	2.133	2.126	2.139	2.151
0.50	2.169	2.173	2.172	2.172	2.157	2.157	2.150	2.163	2.173
0.60	2.192	2.197	2.197	2.199	2.183	2.183	2.173	2.187	2.199
0.70	2.216	2.221	2.221	2.227	2.211	2.213	2.197	2.213	2.227
0.80	2.240	2.245	2.247	2.269	2.245	2.253	2.226	2.243	2.269
0.85	2.252	2.258	2.262	2.306	2.270	2.284	2.247	2.265	2.306
0.90	2.265	2.272	2.282	2.381	2.325	2.345	2.265	2.304	2.381
0.92	2.271	2.278	2.294	2.433	2.369	2.392	2.271	2.333	2.433
0.93	2.274	2.281	2.301	2.467	2.399	2.425	2.274	2.354	2.467
0.94	2.277	2.285	2.311	2.509	2.436	2.461	2.277	2.378	2.509
0.95	2.280	2.290	2.325	2.553	2.477	2.503	2.280	2.407	2.553
0.96	2.285	2.296	2.345	2.610	2.524	2.553	2.285	2.442	2.610
0.97	2.290	2.305	2.380	2.687	2.580	2.617	2.290	2.486	2.687
0.98	2.298	2.322	2.452	2.803	2.657	2.708	2.298	2.550	2.803
0.99	2.322	2.373	2.613	2.998	2.792	2.865	2.322	2.666	2.998

Table 4. Cumulative Distributions of Zenith Atmospheric Noise Temperature at X-Band for Goldstone DSCC, K

CD	January	February	March	April	May	June
0.00	2.140	2.140	2.140	2.140	2.140	2.140
0.10	2.233	2.220	2.232	2.248	2.274	2.278
0.20	2.284	2.268	2.284	2.297	2.330	2.339
0.25	2.306	2.290	2.309	2.320	2.355	2.367
0.30	2.328	2.315	2.333	2.342	2.379	2.394
0.40	2.372	2.363	2.376	2.384	2.426	2.450
0.50	2.419	2.410	2.416	2.423	2.474	2.515
0.60	2.469	2.462	2.458	2.468	2.532	2.582
0.70	2.532	2.527	2.505	2.518	2.599	2.676
0.80	2.640	2.624	2.571	2.575	2.688	2.786
0.85	2.718	2.700	2.613	2.613	2.750	2.845
0.90	2.838	2.840	2.674	2.662	2.839	2.919
0.92	2.949	2.979	2.712	2.690	2.890	2.962
0.93	3.040	3.091	2.743	2.707	2.929	2.990
0.94	3.158	3.246	2.772	2.728	2.977	3.022
0.95	3.340	3.454	2.819	2.759	3.046	3.067
0.96	3.563	3.713	2.910	2.807	3.137	3.148
0.97	3.897	4.123	3.075	2.891	3.299	3.266
0.98	4.479	4.771	3.335	3.083	3.693	3.576
0.99	5.770	6.042	4.104	3.698	4.203	4.329

Table 4 (Cont'd). Cumulative Distributions of Zenith Atmospheric Noise Temperature at X-Band for Goldstone DSCC, K

CD	July	August	September	October	November	December	Minimum	Year Average	Maximum
0.00	2.140	2.140	2.140	2.140	2.140	2.140	2.140	2.140	2.140
0.10	2.313	2.315	2.305	2.275	2.230	2.229	2.220	2.263	2.315
0.20	2.404	2.405	2.369	2.343	2.284	2.279	2.268	2.324	2.405
0.25	2.447	2.443	2.396	2.369	2.309	2.302	2.290	2.352	2.447
0.30	2.484	2.482	2.424	2.394	2.337	2.324	2.315	2.378	2.484
0.40	2.555	2.586	2.485	2.441	2.390	2.367	2.363	2.433	2.586
0.50	2.643	2.682	2.562	2.492	2.445	2.412	2.410	2.492	2.682
0.60	2.776	2.786	2.650	2.545	2.510	2.465	2.458	2.559	2.786
0.70	2.917	2.895	2.782	2.609	2.583	2.534	2.505	2.641	2.917
0.80	3.036	3.004	2.931	2.695	2.688	2.623	2.571	2.739	3.036
0.85	3.105	3.084	3.002	2.744	2.756	2.689	2.613	2.803	3.105
0.90	3.186	3.186	3.105	2.827	2.852	2.789	2.662	2.894	3.186
0.92	3.226	3.229	3.155	2.880	2.921	2.846	2.690	2.953	3.229
0.93	3.256	3.259	3.183	2.910	2.952	2.888	2.707	2.995	3.259
0.94	3.294	3.296	3.215	2.947	2.986	2.963	2.728	3.049	3.296
0.95	3.347	3.334	3.255	2.990	3.025	3.075	2.759	3.125	3.454
0.96	3.413	3.394	3.303	3.052	3.108	3.264	2.807	3.232	3.713
0.97	3.510	3.495	3.393	3.151	3.308	3.523	2.891	3.408	4.123
0.98	3.730	3.730	3.620	3.437	3.733	4.002	3.083	3.761	4.771
0.99	4.267	3.921	4.342	4.180	4.702	5.211	3.698	4.557	6.042

Table 5. Cumulative Distributions of Zenith Atmospheric Noise Temperature at X-Band for Canberra DSCC, K

CD	January	February	March	April	May	June
0.00	2.280	2.280	2.280	2.280	2.280	2.280
0.10	2.612	2.759	2.660	2.589	2.514	2.478
0.20	2.726	2.886	2.769	2.689	2.586	2.536
0.25	2.773	2.940	2.813	2.722	2.616	2.564
0.30	2.817	3.000	2.858	2.754	2.646	2.589
0.40	2.908	3.114	2.947	2.823	2.701	2.648
0.50	3.002	3.232	3.051	2.911	2.759	2.717
0.60	3.111	3.361	3.163	3.006	2.822	2.806
0.70	3.241	3.542	3.290	3.108	2.908	2.915
0.80	3.433	3.851	3.483	3.242	3.063	3.049
0.85	3.561	4.072	3.623	3.346	3.204	3.145
0.90	3.780	4.423	3.853	3.557	3.468	3.338
0.92	3.900	4.717	3.964	3.726	3.666	3.518
0.93	3.990	5.026	4.038	3.852	3.792	3.665
0.94	4.126	5.473	4.154	4.058	3.941	3.824
0.95	4.311	6.070	4.351	4.300	4.153	4.120
0.96	4.599	7.000	4.652	4.574	4.451	4.599
0.97	5.044	8.080	5.143	5.054	4.888	5.280
0.98	6.036	9.861	5.935	5.993	5.734	6.113
0.99	8.100	13.760	7.990	7.410	7.243	7.447

Table 5 (Cont'd). Cumulative Distributions of Zenith Atmospheric Noise Temperature at X-Band for Canberra DSCC, K

CD	July	August	September	October	November	December	Minimum	Year Average	Maximum
0.00	2.280	2.280	2.280	2.280	2.280	2.280	2.280	2.280	2.280
0.10	2.462	2.463	2.490	2.508	2.592	2.580	2.462	2.558	2.759
0.20	2.521	2.521	2.564	2.595	2.680	2.685	2.521	2.645	2.886
0.25	2.548	2.548	2.597	2.631	2.723	2.732	2.548	2.682	2.940
0.30	2.574	2.573	2.629	2.663	2.766	2.779	2.573	2.719	3.000
0.40	2.624	2.625	2.693	2.727	2.851	2.871	2.624	2.792	3.114
0.50	2.683	2.675	2.761	2.794	2.943	2.972	2.675	2.873	3.232
0.60	2.751	2.732	2.836	2.871	3.073	3.089	2.732	2.966	3.361
0.70	2.836	2.809	2.932	2.981	3.246	3.223	2.809	3.083	3.542
0.80	2.951	2.926	3.056	3.175	3.495	3.446	2.926	3.260	3.851
0.85	3.043	3.022	3.165	3.356	3.703	3.632	3.022	3.402	4.072
0.90	3.217	3.254	3.358	3.695	4.170	3.986	3.217	3.670	4.423
0.92	3.340	3.452	3.523	3.957	4.568	4.254	3.340	3.877	4.717
0.93	3.425	3.589	3.638	4.144	4.835	4.443	3.425	4.030	5.026
0.94	3.547	3.777	3.782	4.381	5.149	4.733	3.547	4.237	5.473
0.95	3.711	4.046	3.992	4.700	5.644	5.097	3.711	4.531	6.070
0.96	3.941	4.426	4.346	5.104	6.335	5.720	3.941	4.965	7.000
0.97	4.261	5.095	4.907	5.747	7.360	6.600	4.261	5.605	8.080
0.98	4.691	5.959	5.753	6.809	8.642	7.823	4.691	6.591	9.861
0.99	5.775	7.795	8.178	9.251	11.105	10.220	5.775	8.661	13.760

Table 6. Cumulative Distributions of Zenith Atmospheric Noise Temperature at X-Band for Madrid DSCC, K

CD	January	February	March	April	May	June
0.00	2.239	2.239	2.239	2.239	2.239	2.239
0.10	2.299	2.316	2.361	2.396	2.483	2.507
0.20	2.362	2.379	2.437	2.464	2.561	2.597
0.25	2.392	2.407	2.471	2.494	2.596	2.634
0.30	2.420	2.435	2.506	2.522	2.629	2.670
0.40	2.478	2.490	2.573	2.580	2.699	2.742
0.50	2.546	2.545	2.646	2.642	2.772	2.813
0.60	2.624	2.611	2.724	2.722	2.845	2.884
0.70	2.737	2.693	2.833	2.814	2.937	2.973
0.80	2.924	2.835	3.034	2.927	3.062	3.072
0.85	3.136	2.991	3.281	3.061	3.194	3.128
0.90	3.719	3.465	3.871	3.416	3.550	3.200
0.92	4.313	3.835	4.326	3.743	3.898	3.237
0.93	4.798	4.125	4.643	3.968	4.132	3.264
0.94	5.338	4.531	5.019	4.284	4.446	3.304
0.95	5.910	5.045	5.478	4.709	4.881	3.357
0.96	6.559	5.573	6.102	5.294	5.447	3.461
0.97	7.266	6.254	6.851	5.974	6.090	3.682
0.98	8.174	7.023	7.831	6.896	6.978	4.167
0.99	9.587	8.456	9.371	8.261	8.536	5.578

Table 6 (Cont'd). Cumulative Distributions of Zenith Atmospheric Noise Temperature at X-Band for Madrid DSCC, K

CD	July	August	September	October	November	December	Minimum	Year Average	Maximum
0.00	2.239	2.239	2.239	2.239	2.239	2.239	2.239	2.239	2.239
0.10	2.533	2.566	2.514	2.477	2.366	2.352	2.299	2.431	2.566
0.20	2.618	2.661	2.601	2.583	2.441	2.425	2.362	2.511	2.661
0.25	2.653	2.700	2.638	2.627	2.476	2.458	2.392	2.546	2.700
0.30	2.685	2.737	2.677	2.668	2.509	2.492	2.420	2.580	2.737
0.40	2.748	2.805	2.763	2.750	2.571	2.563	2.478	2.648	2.805
0.50	2.809	2.867	2.850	2.849	2.651	2.646	2.545	2.721	2.867
0.60	2.874	2.936	2.931	2.963	2.752	2.751	2.611	2.803	2.963
0.70	2.944	3.012	3.012	3.093	2.873	2.906	2.693	2.904	3.093
0.80	3.019	3.095	3.120	3.415	3.089	3.191	2.835	3.067	3.415
0.85	3.064	3.142	3.193	3.790	3.305	3.489	2.991	3.234	3.790
0.90	3.117	3.200	3.335	4.664	3.911	4.179	3.117	3.639	4.664
0.92	3.143	3.234	3.452	5.309	4.451	4.768	3.143	3.980	5.309
0.93	3.157	3.257	3.527	5.740	4.838	5.178	3.157	4.224	5.740
0.94	3.173	3.286	3.636	6.275	5.303	5.640	3.173	4.526	6.275
0.95	3.195	3.324	3.788	6.837	5.824	6.167	3.195	4.883	6.837
0.96	3.227	3.383	4.033	7.557	6.419	6.806	3.227	5.329	7.557
0.97	3.276	3.481	4.475	8.548	7.141	7.635	3.276	5.898	8.548
0.98	3.354	3.683	5.421	10.049	8.138	8.808	3.354	6.722	10.049
0.99	3.658	4.342	7.529	12.570	9.886	10.845	3.658	8.233	12.570

Table 7. Cumulative Distributions of Zenith Atmospheric Noise Temperature at Ka-Band for Goldstone DSCC, K

CD	January	February	March	April	May	June
0.00	6.693	6.693	6.693	6.693	6.693	6.693
0.10	7.776	7.591	7.766	7.991	8.362	8.407
0.20	8.266	8.036	8.271	8.453	8.920	9.046
0.25	8.465	8.243	8.505	8.660	9.155	9.317
0.30	8.656	8.478	8.729	8.856	9.371	9.584
0.40	9.046	8.922	9.107	9.215	9.803	10.140
0.50	9.481	9.359	9.443	9.536	10.248	10.823
0.60	9.947	9.850	9.800	9.935	10.832	11.534
0.70	10.608	10.537	10.236	10.414	11.546	12.618
0.80	11.893	11.674	10.923	10.985	12.555	13.927
0.85	12.863	12.618	11.407	11.407	13.311	14.620
0.90	14.415	14.448	12.145	11.969	14.431	15.535
0.92	15.906	16.313	12.624	12.322	15.093	16.079
0.93	17.126	17.824	13.032	12.532	15.612	16.451
0.94	18.719	19.917	13.414	12.795	16.238	16.859
0.95	21.173	22.711	14.041	13.211	17.174	17.462
0.96	24.139	26.139	15.277	13.850	18.391	18.542
0.97	28.557	31.502	17.518	14.999	20.574	20.123
0.98	36.075	39.779	21.032	17.612	25.837	24.276
0.99	52.056	55.298	31.227	25.884	32.510	34.135

Table 7 (Cont'd). Cumulative Distributions of Zenith Atmospheric Noise Temperature at Ka-Band for Goldstone DSCC, K

CD	July	August	September	October	November	December	Minimum	Year Average	Maximum
0.00	6.693	6.693	6.693	6.693	6.693	6.693	6.693	6.693	6.693
0.10	8.902	8.935	8.798	8.378	7.734	7.715	7.591	8.200	8.935
0.20	9.963	9.965	9.460	9.099	8.262	8.195	8.036	8.834	9.965
0.25	10.442	10.389	9.733	9.352	8.511	8.404	8.243	9.105	10.442
0.30	10.845	10.818	10.002	9.585	8.784	8.608	8.478	9.367	10.845
0.40	11.606	12.047	10.630	10.018	9.298	8.977	8.922	9.909	12.047
0.50	12.606	13.157	11.490	10.501	9.848	9.377	9.359	10.498	13.157
0.60	14.231	14.369	12.484	11.023	10.535	9.892	9.800	11.214	14.369
0.70	15.947	15.642	14.091	11.692	11.322	10.642	10.236	12.120	15.947
0.80	17.361	16.922	15.919	12.663	12.559	11.657	10.923	13.264	17.361
0.85	18.195	17.910	16.794	13.230	13.394	12.462	11.407	14.028	18.195
0.90	19.186	19.194	18.082	14.266	14.609	13.743	11.969	15.175	19.194
0.92	19.695	19.731	18.723	14.959	15.522	14.480	12.322	15.955	19.731
0.93	20.072	20.119	19.086	15.348	15.930	15.041	12.532	16.510	20.119
0.94	20.569	20.590	19.500	15.834	16.365	16.055	12.795	17.227	20.590
0.95	21.263	21.085	20.019	16.400	16.878	17.565	13.211	18.230	22.711
0.96	22.130	21.881	20.648	17.234	17.994	20.124	13.850	19.668	26.139
0.97	23.409	23.216	21.839	18.562	20.700	23.583	14.999	22.006	31.502
0.98	26.327	26.321	24.866	22.420	26.362	29.909	17.612	26.674	39.779
0.99	33.332	28.826	34.303	32.203	38.890	45.249	25.884	36.895	55.298

Table 8. Cumulative Distributions of Zenith Atmospheric Noise Temperature at Ka-Band for Canberra DSCL, K

CD	January	February	March	April	May	June
0.00	7.173	7.173	7.173	7.173	7.173	7.173
0.10	11.603	13.634	12.264	11.280	10.235	9.722
0.20	12.937	15.155	13.545	12.430	10.998	10.300
0.25	13.476	15.775	14.029	12.769	11.290	10.559
0.30	13.959	16.483	14.534	13.091	11.585	10.797
0.40	14.990	17.800	15.517	13.805	12.116	11.379
0.50	16.043	19.175	16.707	14.783	12.681	12.097
0.60	17.301	20.691	18.014	15.855	13.317	13.091
0.70	18.841	22.905	19.508	17.026	14.272	14.372
0.80	21.210	26.790	21.887	18.625	16.165	15.980
0.85	22.820	29.600	23.650	19.926	17.988	17.184
0.90	25.635	34.051	26.598	22.655	21.454	19.693
0.92	27.179	37.770	28.028	24.869	24.065	22.089
0.93	28.341	41.642	28.982	26.525	25.724	24.031
0.94	30.108	47.155	30.476	29.218	27.675	26.133
0.95	32.494	54.337	33.018	32.347	30.434	30.012
0.96	36.176	65.123	36.865	35.864	34.280	36.178
0.97	41.786	77.065	43.028	41.910	39.831	44.728
0.98	53.880	95.413	52.675	53.365	50.253	54.798
0.99	77.263	130.360	76.073	69.706	67.836	70.112

Table 8 (Cont'd). Cumulative Distributions of Zenith Atmospheric Noise Temperature at Ka-Band for Canberra DSCL, K

CD	July	August	September	October	November	December	Minimum	Year Average	Maximum
0.00	7.173	7.173	7.173	7.173	7.173	7.173	7.173	7.173	7.173
0.10	9.500	9.508	9.891	10.146	11.322	11.149	9.500	10.837	13.634
0.20	10.084	10.086	10.690	11.126	12.307	12.374	10.084	11.815	15.155
0.25	10.338	10.335	11.024	11.503	12.781	12.908	10.335	12.211	15.775
0.30	10.578	10.577	11.358	11.830	13.257	13.437	10.577	12.600	16.483
0.40	11.037	11.057	12.003	12.481	14.203	14.475	11.037	13.378	17.800
0.50	11.625	11.510	12.717	13.172	15.233	15.630	11.510	14.251	19.175
0.60	12.328	12.073	13.514	14.002	16.781	17.002	12.073	15.296	20.691
0.70	13.273	12.902	14.604	15.278	18.907	18.590	12.902	16.665	22.905
0.80	14.628	14.275	16.078	17.707	22.045	21.393	14.275	18.847	26.790
0.85	15.775	15.495	17.448	20.055	24.715	23.775	15.495	20.645	29.600
0.90	18.046	18.550	19.965	24.499	30.767	28.356	18.046	24.125	34.051
0.92	19.674	21.195	22.148	27.930	35.869	31.821	19.674	26.811	37.770
0.93	20.801	23.012	23.680	30.370	39.234	34.243	20.801	28.792	41.642
0.94	22.435	25.505	25.576	33.424	43.160	37.930	22.435	31.455	47.155
0.95	24.607	29.035	28.334	37.489	49.220	42.486	24.607	35.178	54.337
0.96	27.641	33.961	32.924	42.553	57.451	50.119	27.641	40.580	65.123
0.97	31.799	42.423	40.067	50.431	69.169	60.521	31.799	48.344	77.065
0.98	37.318	52.962	50.490	62.925	83.025	74.270	37.318	59.845	95.413
0.99	50.740	73.948	78.101	89.309	107.318	98.925	50.740	82.126	130.360

Table 9. Cumulative Distributions of Zenith Atmospheric Noise Temperature at Ka-Band for Madrid DSCC, K

CD	January	February	March	April	May	June
0.00	7.031	7.031	7.031	7.031	7.031	7.031
0.10	7.633	7.877	8.517	9.004	10.228	10.570
0.20	8.284	8.522	9.342	9.727	11.083	11.585
0.25	8.585	8.805	9.705	10.021	11.449	11.985
0.30	8.867	9.083	10.068	10.295	11.799	12.368
0.40	9.442	9.611	10.774	10.871	12.527	13.125
0.50	10.161	10.150	11.558	11.502	13.303	13.884
0.60	11.010	10.828	12.403	12.377	14.082	14.632
0.70	12.353	11.732	13.684	13.421	15.129	15.614
0.80	14.705	13.483	16.229	14.754	16.608	16.754
0.85	17.506	15.523	19.494	16.487	18.307	17.404
0.90	25.262	21.866	27.281	21.209	23.006	18.267
0.92	33.016	26.764	33.180	25.536	27.601	18.732
0.93	39.186	30.557	37.221	28.499	30.648	19.078
0.94	45.905	35.775	41.954	32.593	34.688	19.597
0.95	52.827	42.249	47.607	38.023	40.204	20.297
0.96	60.451	48.739	55.094	45.330	47.202	21.680
0.97	68.489	56.871	63.798	53.559	54.940	24.616
0.98	78.415	65.740	74.717	64.299	65.233	30.990
0.99	93.026	81.411	90.853	79.343	82.248	48.751

Table 9 (Cont'd). Cumulative Distributions of Zenith Atmospheric Noise Temperature at Ka-Band for Madrid DSCC, K

CD	July	August	September	October	November	December	Minimum	Year Average	Maximum
0.00	7.031	7.031	7.031	7.031	7.031	7.031	7.031	7.031	7.031
0.10	10.932	11.390	10.663	10.139	8.591	8.381	7.633	9.504	11.390
0.20	11.870	12.469	11.642	11.385	9.403	9.174	8.284	10.385	12.469
0.25	12.242	12.894	12.039	11.879	9.776	9.521	8.585	10.754	12.894
0.30	12.579	13.289	12.468	12.342	10.111	9.877	8.867	11.108	13.289
0.40	13.216	13.997	13.425	13.238	10.743	10.630	9.442	11.814	13.997
0.50	13.819	14.622	14.387	14.369	11.630	11.562	10.150	12.594	14.622
0.60	14.490	15.337	15.278	15.716	12.799	12.777	10.828	13.494	15.716
0.70	15.221	16.163	16.161	17.272	14.234	14.702	11.732	14.660	17.272
0.80	16.022	17.064	17.408	21.411	16.978	18.373	13.483	16.675	21.411
0.85	16.530	17.597	18.294	26.321	19.815	22.304	15.523	18.832	26.321
0.90	17.137	18.268	20.111	37.550	27.806	31.318	17.137	24.131	37.550
0.92	17.439	18.685	21.644	45.586	34.791	38.835	17.439	28.533	45.586
0.93	17.615	18.973	22.632	50.816	39.693	43.947	17.615	31.625	50.816
0.94	17.816	19.349	24.075	57.165	45.478	49.587	17.816	35.382	57.165
0.95	18.090	19.850	26.073	63.655	51.799	55.883	18.090	39.756	63.655
0.96	18.505	20.618	29.290	71.737	58.820	63.298	18.505	45.105	71.737
0.97	19.150	21.920	34.997	82.386	67.080	72.579	19.150	51.733	82.386
0.98	20.181	24.610	46.848	97.580	78.034	85.102	20.181	61.008	97.580
0.99	24.256	33.242	71.396	120.686	95.983	105.191	24.256	77.204	120.686

Table 10. Cumulative Distributions of Zenith Atmospheric Attenuation at L- and S-Bands for Goldstone DSCC, dB

CD	January	February	March	April	May	June
0.00	0.033	0.033	0.033	0.033	0.033	0.033
0.10	0.033	0.033	0.033	0.033	0.033	0.033
0.20	0.033	0.033	0.033	0.033	0.033	0.033
0.25	0.033	0.033	0.033	0.033	0.034	0.034
0.30	0.033	0.033	0.033	0.033	0.034	0.034
0.40	0.033	0.033	0.033	0.033	0.034	0.034
0.50	0.034	0.034	0.034	0.034	0.034	0.034
0.60	0.034	0.034	0.034	0.034	0.034	0.034
0.70	0.034	0.034	0.034	0.034	0.034	0.034
0.80	0.034	0.034	0.034	0.034	0.034	0.034
0.85	0.034	0.034	0.034	0.034	0.034	0.034
0.90	0.034	0.034	0.034	0.034	0.034	0.034
0.92	0.034	0.034	0.034	0.034	0.034	0.034
0.93	0.034	0.034	0.034	0.034	0.034	0.034
0.94	0.034	0.034	0.034	0.034	0.034	0.034
0.95	0.034	0.035	0.034	0.034	0.034	0.034
0.96	0.035	0.035	0.034	0.034	0.034	0.034
0.97	0.035	0.035	0.034	0.034	0.034	0.034
0.98	0.036	0.036	0.034	0.034	0.035	0.035
0.99	0.037	0.038	0.035	0.035	0.035	0.036

Table 10 (Cont'd). Cumulative Distributions of Zenith Atmospheric Attenuation at L- and S-Bands for Goldstone DSCC, dB

CD	July	August	September	October	November	December	Minimum	Year Average	Maximum
0.00	0.033	0.033	0.033	0.033	0.033	0.033	0.033	0.033	0.033
0.10	0.033	0.033	0.033	0.033	0.033	0.033	0.033	0.033	0.033
0.20	0.034	0.034	0.034	0.034	0.033	0.033	0.033	0.033	0.034
0.25	0.034	0.034	0.034	0.034	0.033	0.033	0.033	0.033	0.034
0.30	0.034	0.034	0.034	0.034	0.033	0.033	0.033	0.034	0.034
0.40	0.034	0.034	0.034	0.034	0.034	0.033	0.033	0.034	0.034
0.50	0.034	0.034	0.034	0.034	0.034	0.034	0.034	0.034	0.034
0.60	0.034	0.034	0.034	0.034	0.034	0.034	0.034	0.034	0.034
0.70	0.034	0.034	0.034	0.034	0.034	0.034	0.034	0.034	0.034
0.80	0.034	0.034	0.034	0.034	0.034	0.034	0.034	0.034	0.034
0.85	0.034	0.034	0.034	0.034	0.034	0.034	0.034	0.034	0.034
0.90	0.034	0.034	0.034	0.034	0.034	0.034	0.034	0.034	0.034
0.92	0.034	0.034	0.034	0.034	0.034	0.034	0.034	0.034	0.034
0.93	0.034	0.034	0.034	0.034	0.034	0.034	0.034	0.034	0.034
0.94	0.034	0.034	0.034	0.034	0.034	0.034	0.034	0.034	0.034
0.95	0.034	0.034	0.034	0.034	0.034	0.034	0.034	0.034	0.035
0.96	0.035	0.035	0.034	0.034	0.034	0.034	0.034	0.034	0.035
0.97	0.035	0.035	0.035	0.034	0.034	0.035	0.034	0.035	0.035
0.98	0.035	0.035	0.035	0.035	0.035	0.035	0.034	0.035	0.036
0.99	0.036	0.035	0.036	0.035	0.036	0.037	0.035	0.036	0.038

Table 11. Cumulative Distributions of Zenith Atmospheric Attenuation at L- and S-Bands for Canberra DSAC, dB

CD	January	February	March	April	May	June
0.00	0.036	0.036	0.036	0.036	0.036	0.036
0.10	0.036	0.036	0.036	0.036	0.036	0.036
0.20	0.036	0.036	0.036	0.036	0.036	0.036
0.25	0.036	0.036	0.036	0.036	0.036	0.036
0.30	0.036	0.036	0.036	0.036	0.036	0.036
0.40	0.036	0.036	0.036	0.036	0.036	0.036
0.50	0.036	0.037	0.036	0.036	0.036	0.036
0.60	0.036	0.037	0.036	0.036	0.036	0.036
0.70	0.036	0.037	0.037	0.036	0.036	0.036
0.80	0.037	0.037	0.037	0.036	0.036	0.036
0.85	0.037	0.037	0.037	0.037	0.036	0.036
0.90	0.037	0.038	0.037	0.037	0.037	0.037
0.92	0.037	0.038	0.037	0.037	0.037	0.037
0.93	0.037	0.038	0.037	0.037	0.037	0.037
0.94	0.037	0.039	0.037	0.037	0.037	0.037
0.95	0.038	0.040	0.038	0.038	0.037	0.037
0.96	0.038	0.041	0.038	0.038	0.038	0.038
0.97	0.038	0.042	0.039	0.038	0.038	0.039
0.98	0.040	0.044	0.040	0.040	0.039	0.040
0.99	0.042	0.049	0.042	0.041	0.041	0.041

Table 11 (Cont'd). Cumulative Distributions of Zenith Atmospheric Attenuation at L- and S-Bands for Canberra DSAC, dB

CD	July	August	September	October	November	December	Minimum	Year Average	Maximum
0.00	0.036	0.036	0.036	0.036	0.036	0.036	0.036	0.036	0.036
0.10	0.036	0.036	0.036	0.036	0.036	0.036	0.036	0.036	0.036
0.20	0.036	0.036	0.036	0.036	0.036	0.036	0.036	0.036	0.036
0.25	0.036	0.036	0.036	0.036	0.036	0.036	0.036	0.036	0.036
0.30	0.036	0.036	0.036	0.036	0.036	0.036	0.036	0.036	0.036
0.40	0.036	0.036	0.036	0.036	0.036	0.036	0.036	0.036	0.036
0.50	0.036	0.036	0.036	0.036	0.036	0.036	0.036	0.036	0.037
0.60	0.036	0.036	0.036	0.036	0.036	0.036	0.036	0.036	0.037
0.70	0.036	0.036	0.036	0.036	0.036	0.036	0.036	0.036	0.037
0.80	0.036	0.036	0.036	0.036	0.037	0.037	0.036	0.036	0.037
0.85	0.036	0.036	0.036	0.037	0.037	0.037	0.036	0.037	0.037
0.90	0.036	0.036	0.037	0.037	0.037	0.037	0.036	0.037	0.038
0.92	0.037	0.037	0.037	0.037	0.038	0.038	0.037	0.037	0.038
0.93	0.037	0.037	0.037	0.037	0.038	0.038	0.037	0.037	0.038
0.94	0.037	0.037	0.037	0.038	0.039	0.038	0.037	0.038	0.039
0.95	0.037	0.037	0.037	0.038	0.039	0.039	0.037	0.038	0.040
0.96	0.037	0.038	0.038	0.039	0.040	0.039	0.037	0.038	0.041
0.97	0.038	0.039	0.038	0.039	0.041	0.040	0.038	0.039	0.042
0.98	0.038	0.040	0.039	0.041	0.043	0.042	0.038	0.040	0.044
0.99	0.039	0.042	0.042	0.043	0.046	0.045	0.039	0.043	0.049

Table 12. Cumulative Distributions of Zenith Atmospheric Attenuation at L- and S-Bands for Madrid DSCC, dB

CD	January	February	March	April	May	June
0.00	0.035	0.035	0.035	0.035	0.035	0.035
0.10	0.035	0.035	0.035	0.035	0.035	0.035
0.20	0.035	0.035	0.035	0.035	0.035	0.035
0.25	0.035	0.035	0.035	0.035	0.035	0.035
0.30	0.035	0.035	0.035	0.035	0.035	0.035
0.40	0.035	0.035	0.035	0.035	0.035	0.035
0.50	0.035	0.035	0.035	0.035	0.035	0.035
0.60	0.035	0.035	0.035	0.035	0.035	0.035
0.70	0.035	0.035	0.035	0.035	0.035	0.035
0.80	0.035	0.035	0.036	0.035	0.036	0.036
0.85	0.036	0.035	0.036	0.036	0.036	0.036
0.90	0.036	0.036	0.036	0.036	0.036	0.036
0.92	0.037	0.036	0.037	0.036	0.037	0.036
0.93	0.038	0.037	0.037	0.037	0.037	0.036
0.94	0.038	0.037	0.038	0.037	0.037	0.036
0.95	0.039	0.038	0.038	0.037	0.038	0.036
0.96	0.040	0.038	0.039	0.038	0.038	0.036
0.97	0.040	0.039	0.040	0.039	0.039	0.036
0.98	0.042	0.040	0.041	0.040	0.040	0.037
0.99	0.043	0.042	0.043	0.042	0.042	0.038

Table 12 (Cont'd). Cumulative Distributions of Zenith Atmospheric Attenuation at L- and S-Bands for Madrid DSCC, dB

CD	July	August	September	October	November	December	Minimum	Year Average	Maximum
0.00	0.035	0.035	0.035	0.035	0.035	0.035	0.035	0.035	0.035
0.10	0.035	0.035	0.035	0.035	0.035	0.035	0.035	0.035	0.035
0.20	0.035	0.035	0.035	0.035	0.035	0.035	0.035	0.035	0.035
0.25	0.035	0.035	0.035	0.035	0.035	0.035	0.035	0.035	0.035
0.30	0.035	0.035	0.035	0.035	0.035	0.035	0.035	0.035	0.035
0.40	0.035	0.035	0.035	0.035	0.035	0.035	0.035	0.035	0.035
0.50	0.035	0.035	0.035	0.035	0.035	0.035	0.035	0.035	0.035
0.60	0.035	0.035	0.035	0.036	0.035	0.035	0.035	0.035	0.036
0.70	0.035	0.036	0.036	0.036	0.035	0.035	0.035	0.035	0.036
0.80	0.036	0.036	0.036	0.036	0.036	0.036	0.035	0.036	0.036
0.85	0.036	0.036	0.036	0.036	0.036	0.036	0.035	0.036	0.036
0.90	0.036	0.036	0.036	0.037	0.037	0.037	0.036	0.036	0.037
0.92	0.036	0.036	0.036	0.038	0.037	0.038	0.036	0.037	0.038
0.93	0.036	0.036	0.036	0.039	0.038	0.038	0.036	0.037	0.039
0.94	0.036	0.036	0.036	0.039	0.038	0.039	0.036	0.037	0.039
0.95	0.036	0.036	0.036	0.040	0.039	0.039	0.036	0.038	0.040
0.96	0.036	0.036	0.037	0.041	0.039	0.040	0.036	0.038	0.041
0.97	0.036	0.036	0.037	0.042	0.040	0.041	0.036	0.039	0.042
0.98	0.036	0.036	0.038	0.044	0.041	0.042	0.036	0.040	0.044
0.99	0.036	0.037	0.041	0.047	0.044	0.045	0.036	0.042	0.047

Table 13. Cumulative Distributions of Zenith Atmospheric Attenuation at X-Band  
for Goldstone DSCC, dB

CD	January	February	March	April	May	June
0.00	0.037	0.037	0.037	0.037	0.037	0.037
0.10	0.038	0.038	0.038	0.038	0.039	0.039
0.20	0.038	0.038	0.038	0.039	0.039	0.039
0.25	0.039	0.038	0.039	0.039	0.039	0.040
0.30	0.039	0.038	0.039	0.039	0.040	0.040
0.40	0.039	0.039	0.039	0.039	0.040	0.040
0.50	0.039	0.039	0.039	0.040	0.040	0.041
0.60	0.040	0.040	0.040	0.040	0.041	0.042
0.70	0.041	0.040	0.040	0.040	0.042	0.043
0.80	0.042	0.042	0.041	0.041	0.043	0.044
0.85	0.043	0.043	0.041	0.041	0.043	0.045
0.90	0.045	0.045	0.042	0.042	0.045	0.046
0.92	0.046	0.047	0.043	0.042	0.045	0.047
0.93	0.048	0.049	0.043	0.042	0.046	0.047
0.94	0.050	0.051	0.043	0.043	0.047	0.047
0.95	0.052	0.054	0.044	0.043	0.048	0.048
0.96	0.056	0.058	0.046	0.044	0.049	0.049
0.97	0.061	0.065	0.048	0.045	0.052	0.051
0.98	0.070	0.075	0.052	0.048	0.058	0.056
0.99	0.091	0.095	0.064	0.058	0.066	0.068

Table 13 (Cont'd). Cumulative Distributions of Zenith Atmospheric Attenuation at X-Band  
for Goldstone DSCC, dB

CD	July	August	September	October	November	December	Minimum	Year Average	Maximum
0.00	0.037	0.037	0.037	0.037	0.037	0.037	0.037	0.037	0.037
0.10	0.039	0.039	0.039	0.039	0.038	0.038	0.038	0.038	0.039
0.20	0.040	0.040	0.040	0.039	0.038	0.038	0.038	0.039	0.040
0.25	0.041	0.041	0.040	0.040	0.039	0.038	0.038	0.039	0.041
0.30	0.041	0.041	0.040	0.040	0.039	0.039	0.038	0.040	0.041
0.40	0.042	0.043	0.041	0.040	0.039	0.039	0.039	0.040	0.043
0.50	0.043	0.044	0.042	0.041	0.040	0.039	0.039	0.041	0.044
0.60	0.045	0.045	0.043	0.041	0.041	0.040	0.040	0.041	0.045
0.70	0.047	0.046	0.045	0.042	0.041	0.041	0.040	0.042	0.047
0.80	0.048	0.048	0.047	0.043	0.043	0.042	0.041	0.043	0.048
0.85	0.049	0.049	0.047	0.043	0.044	0.042	0.041	0.044	0.049
0.90	0.050	0.050	0.049	0.044	0.045	0.044	0.042	0.046	0.050
0.92	0.051	0.051	0.050	0.045	0.046	0.045	0.042	0.046	0.051
0.93	0.051	0.051	0.050	0.046	0.046	0.045	0.042	0.047	0.051
0.94	0.052	0.052	0.050	0.046	0.047	0.046	0.043	0.048	0.052
0.95	0.052	0.052	0.051	0.047	0.047	0.048	0.043	0.049	0.054
0.96	0.053	0.053	0.052	0.048	0.049	0.051	0.044	0.051	0.058
0.97	0.055	0.055	0.053	0.049	0.052	0.055	0.045	0.053	0.065
0.98	0.058	0.058	0.057	0.054	0.058	0.063	0.048	0.059	0.075
0.99	0.067	0.061	0.068	0.065	0.074	0.082	0.058	0.071	0.095

Table 14. Cumulative Distributions of Zenith Atmospheric Attenuation at X-Band  
for Canberra DSCC, dB

CD	January	February	March	April	May	June
0.00	0.039	0.039	0.039	0.039	0.039	0.039
0.10	0.044	0.047	0.045	0.044	0.043	0.042
0.20	0.046	0.048	0.047	0.045	0.043	0.043
0.25	0.046	0.049	0.047	0.045	0.044	0.043
0.30	0.047	0.050	0.048	0.046	0.044	0.043
0.40	0.048	0.051	0.049	0.047	0.044	0.044
0.50	0.049	0.053	0.050	0.048	0.045	0.044
0.60	0.050	0.054	0.051	0.049	0.046	0.045
0.70	0.052	0.057	0.053	0.050	0.047	0.047
0.80	0.055	0.061	0.055	0.052	0.049	0.048
0.85	0.056	0.064	0.057	0.053	0.051	0.050
0.90	0.060	0.070	0.061	0.056	0.055	0.053
0.92	0.061	0.074	0.062	0.059	0.058	0.055
0.93	0.063	0.079	0.063	0.061	0.060	0.058
0.94	0.065	0.086	0.065	0.064	0.062	0.060
0.95	0.068	0.096	0.068	0.068	0.065	0.065
0.96	0.072	0.110	0.073	0.072	0.070	0.072
0.97	0.079	0.128	0.081	0.079	0.077	0.083
0.98	0.095	0.156	0.093	0.094	0.090	0.096
0.99	0.128	0.219	0.126	0.117	0.114	0.117

Table 14 (Cont'd). Cumulative Distributions of Zenith Atmospheric Attenuation at X-Band  
for Canberra DSCC, dB

CD	July	August	September	October	November	December	Minimum	Year Average	Maximum
0.00	0.039	0.039	0.039	0.039	0.039	0.039	0.039	0.039	0.039
0.10	0.042	0.042	0.042	0.043	0.044	0.044	0.042	0.043	0.047
0.20	0.042	0.042	0.043	0.044	0.045	0.045	0.042	0.044	0.048
0.25	0.043	0.043	0.043	0.044	0.046	0.046	0.043	0.045	0.049
0.30	0.043	0.043	0.044	0.044	0.046	0.046	0.043	0.045	0.050
0.40	0.043	0.043	0.044	0.045	0.047	0.047	0.043	0.046	0.051
0.50	0.044	0.044	0.045	0.046	0.048	0.049	0.044	0.047	0.053
0.60	0.044	0.044	0.046	0.046	0.050	0.050	0.044	0.048	0.054
0.70	0.045	0.045	0.047	0.048	0.052	0.052	0.045	0.049	0.057
0.80	0.047	0.046	0.049	0.050	0.056	0.055	0.046	0.052	0.061
0.85	0.048	0.048	0.050	0.053	0.059	0.057	0.048	0.054	0.064
0.90	0.051	0.051	0.053	0.058	0.066	0.063	0.051	0.058	0.070
0.92	0.052	0.054	0.055	0.062	0.072	0.067	0.052	0.061	0.074
0.93	0.054	0.056	0.057	0.065	0.076	0.070	0.054	0.063	0.079
0.94	0.056	0.059	0.059	0.069	0.081	0.074	0.056	0.067	0.086
0.95	0.058	0.063	0.063	0.074	0.089	0.080	0.058	0.071	0.096
0.96	0.062	0.069	0.068	0.080	0.100	0.090	0.062	0.078	0.110
0.97	0.067	0.080	0.077	0.090	0.116	0.104	0.067	0.088	0.128
0.98	0.074	0.094	0.090	0.107	0.136	0.123	0.074	0.104	0.156
0.99	0.091	0.123	0.129	0.146	0.176	0.162	0.091	0.137	0.219

Table 15. Cumulative Distributions of Zenith Atmospheric Attenuation at X-Band  
for Madrid DSCC, dB

CD	January	February	March	April	May	June
0.00	0.038	0.038	0.038	0.038	0.038	0.038
0.10	0.039	0.039	0.040	0.041	0.042	0.042
0.20	0.040	0.040	0.041	0.041	0.043	0.044
0.25	0.040	0.040	0.041	0.042	0.043	0.044
0.30	0.040	0.040	0.042	0.042	0.044	0.044
0.40	0.041	0.041	0.042	0.042	0.044	0.045
0.50	0.042	0.042	0.043	0.043	0.045	0.046
0.60	0.042	0.042	0.044	0.044	0.046	0.047
0.70	0.044	0.043	0.045	0.045	0.047	0.048
0.80	0.046	0.045	0.048	0.046	0.049	0.049
0.85	0.050	0.047	0.052	0.048	0.051	0.049
0.90	0.059	0.055	0.061	0.054	0.056	0.050
0.92	0.068	0.060	0.068	0.059	0.061	0.051
0.93	0.076	0.065	0.073	0.062	0.065	0.051
0.94	0.084	0.071	0.079	0.067	0.070	0.052
0.95	0.093	0.079	0.086	0.074	0.077	0.053
0.96	0.103	0.088	0.096	0.083	0.086	0.054
0.97	0.114	0.098	0.108	0.094	0.096	0.058
0.98	0.129	0.111	0.123	0.109	0.110	0.065
0.99	0.151	0.133	0.148	0.130	0.135	0.087

Table 15 (Cont'd). Cumulative Distributions of Zenith Atmospheric Attenuation at X-Band  
for Madrid DSCC, dB

CD	July	August	September	October	November	December	Minimum	Year Average	Maximum
0.00	0.038	0.038	0.038	0.038	0.038	0.038	0.038	0.038	0.038
0.10	0.043	0.043	0.043	0.042	0.040	0.040	0.039	0.041	0.043
0.20	0.044	0.045	0.044	0.043	0.041	0.041	0.040	0.042	0.045
0.25	0.044	0.045	0.044	0.044	0.041	0.041	0.040	0.043	0.045
0.30	0.045	0.046	0.045	0.044	0.042	0.041	0.040	0.043	0.046
0.40	0.045	0.046	0.046	0.045	0.042	0.042	0.041	0.044	0.046
0.50	0.046	0.047	0.047	0.046	0.043	0.043	0.042	0.044	0.047
0.60	0.046	0.047	0.047	0.048	0.044	0.044	0.042	0.045	0.048
0.70	0.047	0.048	0.048	0.050	0.046	0.047	0.043	0.047	0.050
0.80	0.048	0.049	0.050	0.054	0.049	0.051	0.045	0.049	0.054
0.85	0.048	0.050	0.050	0.060	0.052	0.055	0.047	0.051	0.060
0.90	0.049	0.050	0.053	0.074	0.062	0.066	0.049	0.057	0.074
0.92	0.049	0.051	0.054	0.084	0.070	0.075	0.049	0.063	0.084
0.93	0.050	0.051	0.055	0.091	0.076	0.082	0.050	0.066	0.091
0.94	0.050	0.052	0.057	0.099	0.084	0.089	0.050	0.071	0.099
0.95	0.050	0.052	0.059	0.108	0.092	0.097	0.050	0.077	0.108
0.96	0.051	0.053	0.063	0.119	0.101	0.107	0.051	0.084	0.119
0.97	0.051	0.054	0.070	0.135	0.112	0.120	0.051	0.093	0.135
0.98	0.052	0.058	0.085	0.159	0.128	0.139	0.052	0.106	0.159
0.99	0.057	0.068	0.118	0.200	0.156	0.172	0.057	0.130	0.200

Table 16. Cumulative Distributions of Zenith Atmospheric Attenuation at Ka-Band  
for Goldstone DSCC, dB

CD	January	February	March	April	May	June
0.00	0.116	0.116	0.116	0.116	0.116	0.116
0.10	0.133	0.130	0.133	0.137	0.143	0.144
0.20	0.140	0.136	0.140	0.144	0.152	0.154
0.25	0.143	0.139	0.144	0.146	0.155	0.158
0.30	0.146	0.143	0.147	0.149	0.158	0.162
0.40	0.151	0.149	0.152	0.154	0.164	0.169
0.50	0.157	0.155	0.156	0.158	0.170	0.179
0.60	0.163	0.161	0.161	0.163	0.178	0.190
0.70	0.172	0.171	0.166	0.169	0.188	0.206
0.80	0.192	0.188	0.176	0.177	0.203	0.226
0.85	0.207	0.203	0.183	0.183	0.214	0.236
0.90	0.232	0.232	0.194	0.191	0.232	0.250
0.92	0.256	0.263	0.202	0.197	0.242	0.259
0.93	0.276	0.288	0.208	0.200	0.251	0.265
0.94	0.302	0.322	0.214	0.204	0.261	0.271
0.95	0.343	0.369	0.224	0.211	0.276	0.281
0.96	0.393	0.427	0.245	0.221	0.296	0.299
0.97	0.469	0.520	0.281	0.240	0.332	0.325
0.98	0.600	0.667	0.340	0.283	0.421	0.395
0.99	0.894	0.956	0.514	0.422	0.537	0.565

Table 16 (Cont'd). Cumulative Distributions of Zenith Atmospheric Attenuation at Ka-Band  
for Goldstone DSCC, dB

CD	July	August	September	October	November	December	Minimum	Year Average	Maximum
0.00	0.116	0.116	0.116	0.116	0.116	0.116	0.116	0.116	0.116
0.10	0.153	0.153	0.151	0.144	0.132	0.132	0.130	0.141	0.153
0.20	0.170	0.170	0.161	0.155	0.140	0.139	0.136	0.150	0.170
0.25	0.177	0.176	0.165	0.158	0.144	0.142	0.139	0.154	0.177
0.30	0.183	0.183	0.169	0.162	0.148	0.145	0.143	0.158	0.183
0.40	0.194	0.202	0.178	0.167	0.155	0.150	0.149	0.166	0.202
0.50	0.210	0.219	0.191	0.174	0.163	0.155	0.155	0.174	0.219
0.60	0.235	0.238	0.206	0.181	0.173	0.162	0.161	0.184	0.238
0.70	0.262	0.257	0.231	0.190	0.184	0.173	0.166	0.198	0.262
0.80	0.283	0.276	0.259	0.205	0.203	0.188	0.176	0.215	0.283
0.85	0.296	0.291	0.272	0.213	0.216	0.200	0.183	0.226	0.296
0.90	0.311	0.311	0.293	0.229	0.235	0.221	0.191	0.244	0.311
0.92	0.319	0.320	0.303	0.240	0.250	0.232	0.197	0.257	0.320
0.93	0.325	0.326	0.309	0.246	0.256	0.241	0.200	0.266	0.326
0.94	0.333	0.334	0.315	0.254	0.263	0.258	0.204	0.278	0.334
0.95	0.345	0.342	0.324	0.263	0.271	0.283	0.211	0.294	0.369
0.96	0.359	0.355	0.334	0.277	0.290	0.325	0.221	0.318	0.427
0.97	0.380	0.377	0.354	0.299	0.334	0.383	0.240	0.357	0.520
0.98	0.430	0.430	0.405	0.363	0.430	0.492	0.283	0.437	0.667
0.99	0.551	0.472	0.568	0.531	0.650	0.766	0.422	0.617	0.956

Table 17. Cumulative Distributions of Zenith Atmospheric Attenuation at Ka-Band for Canberra DSCC, dB

CD	January	February	March	April	May	June
0.00	0.124	0.124	0.124	0.124	0.124	0.124
0.10	0.200	0.236	0.212	0.195	0.176	0.167
0.20	0.222	0.261	0.232	0.213	0.188	0.176
0.25	0.230	0.270	0.240	0.218	0.192	0.179
0.30	0.237	0.282	0.247	0.222	0.196	0.182
0.40	0.253	0.302	0.262	0.232	0.203	0.191
0.50	0.269	0.323	0.280	0.247	0.211	0.201
0.60	0.288	0.346	0.300	0.263	0.220	0.216
0.70	0.311	0.381	0.323	0.280	0.234	0.235
0.80	0.349	0.445	0.360	0.305	0.263	0.260
0.85	0.374	0.492	0.389	0.325	0.292	0.279
0.90	0.421	0.569	0.438	0.370	0.349	0.320
0.92	0.447	0.634	0.462	0.407	0.393	0.360
0.93	0.467	0.704	0.478	0.435	0.421	0.392
0.94	0.497	0.806	0.503	0.481	0.455	0.428
0.95	0.538	0.942	0.548	0.536	0.502	0.495
0.96	0.603	1.154	0.615	0.598	0.569	0.603
0.97	0.704	1.402	0.727	0.706	0.668	0.758
0.98	0.930	1.814	0.907	0.920	0.861	0.948
0.99	1.404	2.724	1.378	1.245	1.206	1.253

Table 17 (Cont'd). Cumulative Distributions of Zenith Atmospheric Attenuation at Ka-Band for Canberra DSCC, dB

CD	July	August	September	October	November	December	Minimum	Year Average	Maximum
0.00	0.124	0.124	0.124	0.124	0.124	0.124	0.124	0.124	0.124
0.10	0.163	0.163	0.170	0.175	0.195	0.192	0.163	0.187	0.236
0.20	0.172	0.172	0.182	0.190	0.211	0.212	0.172	0.202	0.261
0.25	0.175	0.175	0.187	0.196	0.218	0.220	0.175	0.208	0.270
0.30	0.179	0.179	0.192	0.200	0.225	0.228	0.179	0.214	0.282
0.40	0.185	0.185	0.201	0.210	0.239	0.244	0.185	0.225	0.302
0.50	0.193	0.191	0.212	0.219	0.255	0.261	0.191	0.238	0.323
0.60	0.203	0.199	0.223	0.231	0.279	0.282	0.199	0.253	0.346
0.70	0.217	0.211	0.239	0.251	0.312	0.307	0.211	0.274	0.381
0.80	0.237	0.232	0.262	0.289	0.363	0.352	0.232	0.309	0.445
0.85	0.255	0.251	0.283	0.327	0.407	0.391	0.251	0.338	0.492
0.90	0.292	0.300	0.324	0.401	0.510	0.468	0.292	0.396	0.569
0.92	0.319	0.344	0.361	0.460	0.600	0.528	0.319	0.441	0.634
0.93	0.337	0.375	0.386	0.502	0.660	0.570	0.337	0.476	0.704
0.94	0.365	0.417	0.418	0.555	0.731	0.636	0.365	0.522	0.806
0.95	0.401	0.478	0.466	0.627	0.844	0.718	0.401	0.589	0.942
0.96	0.453	0.564	0.545	0.719	1.001	0.860	0.453	0.687	1.154
0.97	0.525	0.716	0.673	0.865	1.236	1.061	0.525	0.832	1.402
0.98	0.622	0.912	0.865	1.108	1.531	1.341	0.622	1.058	1.814
0.99	0.869	1.333	1.422	1.670	2.102	1.895	0.869	1.533	2.724

Table 18. Cumulative Distributions of Zenith Atmospheric Attenuation at Ka-Band for Madrid DSCC, dB

CD	January	February	March	April	May	June
0.00	0.121	0.121	0.121	0.121	0.121	0.121
0.10	0.131	0.135	0.146	0.155	0.176	0.182
0.20	0.141	0.145	0.159	0.166	0.189	0.198
0.25	0.145	0.149	0.164	0.170	0.195	0.204
0.30	0.149	0.153	0.170	0.174	0.200	0.210
0.40	0.158	0.160	0.180	0.182	0.210	0.221
0.50	0.168	0.168	0.192	0.191	0.222	0.231
0.60	0.181	0.178	0.204	0.204	0.233	0.242
0.70	0.201	0.191	0.224	0.219	0.248	0.256
0.80	0.239	0.218	0.264	0.239	0.271	0.273
0.85	0.284	0.251	0.318	0.267	0.298	0.283
0.90	0.415	0.356	0.449	0.345	0.376	0.296
0.92	0.549	0.440	0.552	0.418	0.454	0.303
0.93	0.659	0.505	0.624	0.469	0.507	0.308
0.94	0.782	0.597	0.709	0.541	0.578	0.317
0.95	0.913	0.714	0.813	0.637	0.676	0.328
0.96	1.061	0.834	0.955	0.770	0.805	0.351
0.97	1.222	0.989	1.126	0.925	0.951	0.401
0.98	1.430	1.165	1.351	1.135	1.154	0.510
0.99	1.756	1.494	1.705	1.449	1.512	0.832

Table 18 (Cont'd). Cumulative Distributions of Zenith Atmospheric Attenuation at Ka-Band for Madrid DSCC, dB

CD	July	August	September	October	November	December	Minimum	Year Average	Maximum
0.00	0.121	0.121	0.121	0.121	0.121	0.121	0.121	0.121	0.121
0.10	0.188	0.196	0.184	0.174	0.147	0.144	0.131	0.163	0.196
0.20	0.203	0.213	0.199	0.194	0.160	0.156	0.141	0.177	0.213
0.25	0.208	0.220	0.205	0.202	0.166	0.161	0.145	0.183	0.220
0.30	0.213	0.226	0.211	0.209	0.171	0.167	0.149	0.188	0.226
0.40	0.222	0.236	0.226	0.223	0.180	0.178	0.158	0.198	0.236
0.50	0.230	0.244	0.240	0.240	0.193	0.192	0.168	0.210	0.244
0.60	0.240	0.254	0.253	0.260	0.211	0.211	0.178	0.223	0.260
0.70	0.250	0.266	0.266	0.284	0.233	0.241	0.191	0.240	0.284
0.80	0.261	0.278	0.284	0.352	0.277	0.300	0.218	0.272	0.352
0.85	0.268	0.286	0.298	0.435	0.323	0.366	0.251	0.307	0.435
0.90	0.277	0.296	0.327	0.631	0.459	0.520	0.277	0.396	0.631
0.92	0.281	0.302	0.352	0.778	0.581	0.653	0.281	0.473	0.778
0.93	0.284	0.307	0.368	0.876	0.668	0.747	0.284	0.528	0.876
0.94	0.287	0.313	0.393	0.998	0.774	0.852	0.287	0.596	0.998
0.95	0.291	0.321	0.426	1.126	0.893	0.972	0.291	0.677	1.126
0.96	0.298	0.333	0.482	1.291	1.028	1.118	0.298	0.778	1.291
0.97	0.309	0.355	0.582	1.518	1.193	1.307	0.309	0.907	1.518
0.98	0.325	0.400	0.797	1.865	1.422	1.577	0.325	1.095	1.865
0.99	0.394	0.549	1.280	2.452	1.825	2.048	0.394	1.442	2.452

810-005, Rev. E  
105, Rev. B

Table 19. Monthly and Year-Average Rainfall Amounts at the DSN Antenna Locations

Month	Goldstone		Canberra		Madrid	
	inches	mm	inches	mm	inches	mm
January	1.02	25.9	3.61	91.7	1.48	37.5
February	1.18	30.0	2.74	69.7	1.38	35.0
March	0.90	22.9	2.90	73.6	1.10	28.0
April	0.20	5.1	2.85	72.4	1.87	47.5
May	0.19	4.8	2.94	74.8	1.56	39.5
June	0.04	1.0	2.70	68.7	1.26	32.0
July	0.35	8.9	3.36	85.3	0.57	14.5
August	0.59	15.0	3.90	99.0	0.59	15.0
September	0.39	9.9	3.73	94.7	1.16	29.5
October	0.15	3.8	3.70	94.0	1.54	39.0
November	0.23	5.8	3.50	88.8	2.01	51.0
December	0.57	14.5	2.42	61.4	1.75	44.5
Year Average	5.81	147.6	38.67	982.1	16.26	413.0

Table 20. Parameters for X-Band Planetary Noise Calculation, plus X-Band and Ka-Band Noise Temperatures at Mean Minimum Distance from Earth

Planet	Diameter (km)		Mean Distance from Earth ( $10^6$ km)		Mean Distance from Sun		Blackbody Disk Temp (K)	$T_{\text{Planet}}$ at Mean Minimum Distance (K)		
								X-Band		Ka-Band
	polar	equatorial	min.	max.	( $10^6$ km)	AU		70-m (74.4 dBi gain)	34-m (68.3 dBi gain)	34-m (78.8 dBi gain)
Mercury		4880	91.7	207.5	57.9	0.387	625	3.05	0.75	8.39
Venus		12104	41.4	257.8	108.2	0.723	625 (X-band) 415 (Ka-band)	91.96	22.57	– 253.29
Earth		12757	–	–	149.6	1.000	250–300 <sup>1</sup>	–	–	–
Mars		6794	78.3	377.5	227.9	1.523	180	2.33	0.57	6.43
Jupiter	134102	142984	628.7	927.9	778.3	5.203	152	13.53	3.32	37.27
Saturn	108728	120536	1279.8	1579.0	1429.4	9.555	155	2.37	0.58	6.52
Uranus		51118	2721.4	3020.6	2871.0	19.191	160	0.10	0.02	0.27
Neptune		49532	4354.4	4653.6	4504.0	30.107	160	0.04	0.01	0.10
Pluto		2274	5763.9	6063.1	5913.5	39.529	160	0.00	0.00	0.00

Note:

1. Ocean (250 K) and Land (300 K)